remote sensing

MDPI

Review

Remote Sensing Monitoring of Rice and Wheat Canopy Nitrogen: A Review

Jie Zheng [1,2], Xiaoyu Song [1], Guijun Yang [1], Xiaochu Du [2], Xin Mei [2] and Xiaodong Yang [1,3,*]

[1] Key Laboratory of Quantitative Remote Sensing in Agriculture of Ministry of Agriculture and Rural Affairs, Information Technology Research Center, Beijing Academy of Agriculture and Forestry Sciences, Beijing 100097, China
[2] Faculty of Resources and Environment Science, Hubei University, Wuhan 430062, China
[3] Huanan Industrial Technology Research Institute of Zhejiang University, Guangzhou 510700, China
* Correspondence: yangxd@nercita.org.cn

Abstract: Nitrogen(N) is one of the most important elements for crop growth and yield formation. Insufficient or excessive application of N fertilizers can limit crop yield and quality, especially as excessive N fertilizers can damage the environment and proper fertilizer application is essential for agricultural production. Efficient monitoring of crop N content is the basis of precise fertilizer management, and therefore to increase crop yields and improve crop quality. Remote sensing has gradually replaced traditional destructive methods such as field surveys and laboratory testing for crop N diagnosis. With the rapid advancement of remote sensing, a review on crop N monitoring is badly in need of better summary and discussion. The purpose of this study was to identify current research trends and key issues related to N monitoring. It begins with a comprehensive statistical analysis of the literature on remote sensing monitoring of N in rice and wheat over the past 20 years. The study then elucidates the physiological mechanisms and spectral response characteristics of remote sensing monitoring of canopy N. The following section summarizes the techniques and methods applied in remote sensing monitoring of canopy N from three aspects: remote sensing platforms for N monitoring; correlation between remotely sensed data and N status; and the retrieval methods of N status. The influential factors of N retrieval were then discussed with detailed classification. However, there remain challenges and problems that need to be addressed in the future studies, including the fusion of multisource data from different platforms, and the uncertainty of canopy N inversion in the presence of background factors. The newly developed hybrid model integrates the flexibility of machine learning with the mechanism of physical models. It could be problem solving, which has the advantages of processing multi-source data and reducing the interference of confounding factors. It could be the future development direction of crop N inversion with both high precision and universality.

Keywords: rice and wheat; nitrogen remote sensing; quantitative retrieval; research prospect

Citation: Zheng, J.; Song, X.; Yang, G.; Du, X.; Mei, X.; Yang, X. Remote Sensing Monitoring of Rice and Wheat Canopy Nitrogen: A Review. *Remote Sens.* **2022**, *14*, 5712. https://doi.org/10.3390/rs14225712

Academic Editors: Kenji Omasa, Shan Lu and Jie Wang

Received: 30 September 2022
Accepted: 6 November 2022
Published: 11 November 2022

1. Introduction

The effective guarantee of national food security is a key objective for China. Therefore, it has become a need of green agriculture to reduce the amount and increase the efficiency of chemical fertilizers, which could improve the effective supply of agriculture [1–3]. Rice and wheat are the main crops in the world, with a wide distribution and highly suitability. How to achieve high quality and yield is currently a major challenge for agricultural production [4–6]. N made up more than 40% of the mineral elements needed for the growth of rice and wheat [7]. Its content would impact the physiological traits, photosynthesis, and enzyme activities, leading to variations in protein content and grain production [8–10]. Healthy plants have a total N content that ranges from 0.3% to 5% of their dry matter, which directly affects crop production. N deficiency can hinder chlorophyll (Chl) synthesis

and reduce the effective number of spikes, thus reducing yields. A surplus of N prevents photosynthetic products from reaching the seeds, delaying maturation [7,11]. Therefore, N content during crop growth has become one of the most important indicators in agricultural production management. Currently it is common to use base fertilizer, or top dressing through experience. It will result in too much or not enough N, which not only inhibits crop growth but also pollutes the environment. How to monitor rice and wheat canopy N timely and accurately, so as to guide variable rate fertilization has become a core research issue [12–15].

Currently the experts in plant protection and agronomy test N manually by observing crop symptoms, plant growth and leaf color. They also use chemical diagnostics, such as plant total N diagnostics and rapid nitrate diagnostics, to detect the N content of each organ. The former has variances in results due to subjective judgments. The latter has good accuracy but destroys the plant and has a time lag, making large-scale application difficult [16]. Therefore, traditional N assessment methods do not facilitate variable rate fertilization, because the information on the timing and extent of crop N abundance and deficiency is not efficiently provided. Remote sensing has enabled the rapid development of multiple scales of application, including satellite, unmanned aerial vehicles (UAVs) and ground. It is the current technology for rapidly acquiring spatial and temporal continuum information on a large range. The spectrum is sensitive to the N response in the Visible–Near Infrared (VIS–NIR). This spectral information can show subtle changes in N content, allowing for more accurate N retrieval [17,18]. Remote sensing monitoring of N in rice and wheat can be non-destructive, effective, and real-time for large-scale studies. It offers significant potential for crop nutrient diagnosis and as a basis of subsequent guidance on fertilizer application [19–21].

Both rice and wheat belong to the gramineous cereal crop in the botanical classification, and both are C3 crops with similar photosynthetic systems [22]. Thus, the absorption of colored light by Chl in both canopies is consistent and the response to the spectrum is similar. N is mainly found in the Chl of the photosynthetic systems and the process of N accumulation in rice and wheat has a high degree of similarity [23,24]. They are both transformed into nutrient bodies at the vegetative growth stages and into reproductive organs at the reproductive growth stages, and there are anisotropic changes in N accumulation in each organ at the growth stage [23,25]. Although the cropping patterns differ, one being dryland and the other paddy, this effect can be attenuated when pre-processing the remote sensing data [26]. Therefore, in remote sensing-based studies, the N transformation processes in rice and wheat are highly consistent, making their remote sensing monitoring systems relatively similar [14,27,28]. In this study, the remote sensing monitoring techniques for both crops are explored in an integrated manner.

To analyze and summarize the current research hotspots and trends in the field of remote sensing of canopy N in rice and wheat, this paper traces the related literature in the Web of Science ™ Core Collection Database. The literature is retrieved and filtered by the topics "nitrogen concentration" or "nitrogen content", "rice" or "wheat" and "remote sensing". An initial collection of 572 apparently relevant records covered the period 2003–2021. An initial screening progress is conducted to exclude literature that is not relevant to the review, such as conference proceedings, patents, etc. However, it still contains some irrelevant literature, and a further screening is necessary. This is followed by a more detailed screening on titles and abstracts to exclude the following: (1) non-targeted research topics (e.g., corn, cotton, grassland, etc.); (2) not directly estimated N (e.g., Chl, protein, etc.); (3) estimated other indicators (e.g., leaf area, plant height, yield, etc.); (4) measured soil N or other trace elements in agricultural fields; and (5) review articles. By carefully reading the titles and abstracts, off-topic papers are obviously manually excluded. Eventually, a total of 174 articles were identified and analyzed in depth. Figure 1 shows the number of studies retrieved from 2003 to 2021 that used remotely sensed data to assess the canopy N status of rice and wheat, reflecting the general trend in research on the application of remote sensing monitoring of canopy N.

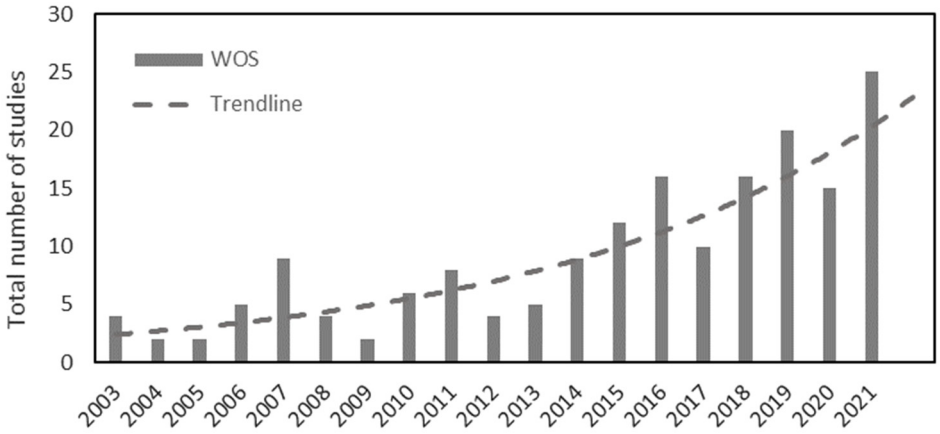

Figure 1. Number of rice and wheat N retrieval research studies per year from 2003 to 2021.

Remote sensing technology has shown great potential for crop N monitoring, providing research ideas from various perspectives. This paper based on the mechanism of remote sensing monitoring of canopy N, respectively summarizes the current techniques and methods from three aspects: remote sensing platforms for canopy N monitoring; correlation between remotely sensed data and N status; and the retrieval methods of N status. Then it discusses the factors affecting the accuracy in remote sensing of canopy N and sketches future areas for research.

2. Mechanisms for Remote Sensing Monitoring of Canopy N

2.1. Physiological Mechanisms of Crop N

Focusing on crop physiological mechanisms, N is closely linked to Chl. N is an important component in the formation of chloroplasts and Rubisco enzymes. Increasing leaf N content will significantly increase leaf chlorophyll content (LCC) and Rubisco enzymes, ultimately leading to a significant increase in crop photosynthetic rate and consequent changes in the external morphology and internal structure of crop leaves [9,29]. Chl can respond to N uptake by crops, and the strength of the relationship directly affects the accuracy of N estimation. However, N is redistributed and reused in the crop during growth. Early in crop development, N is initially concentrated in nutrient bodies such as leaves, and as nutritional and reproductive growth coexist, N starts to be distributed to nutrient bodies and reproductive organs; at the crop maturity stage, N in nutrient bodies is transferred to reproductive organs. This resulted in varying degrees of N and Chl content reduction in the canopy leaves, which changed the correlations between crop N and Chl at various growth stages [25]. In addition to Chl, other mineral deficits, diseases, frost damage, and water stress may also produce leaf yellowing, and using Chl content as a proxy for N is misleading, which limits the ability to estimate N directly from Chl [28]. It has been recommended to utilize leaf protein as a substitute for leaf N content in several studies [30,31], because in contrast to Chl, protein is also a major nitrogenous component in crops and contributes to the varied distribution of N in crop plants. The mechanism of protein–N interactions is under investigation.

2.2. Spectral Response Properties of Canopy N

N affects the spectral reflectance of crops by influencing the Chl content of green crops (Figure 2). Healthy crops' VIS reflectance spectrum is determined by the Chl's absorption effect, which forms a prominent reflectance peak near 550 nm. Multiple reflections in the NIR combine to generate a red edge region of reflectance in the range of 700–780 nm, and the rising slope of the curve reflects the Chl content per unit area to some extent. NIR (780–1350 nm) is closely related to leaf structure and is instructive for exploring whether N is influenced by leaf structure. Under N stress, both the canopy spectral reflectance and the vertical distribution of N will alter.

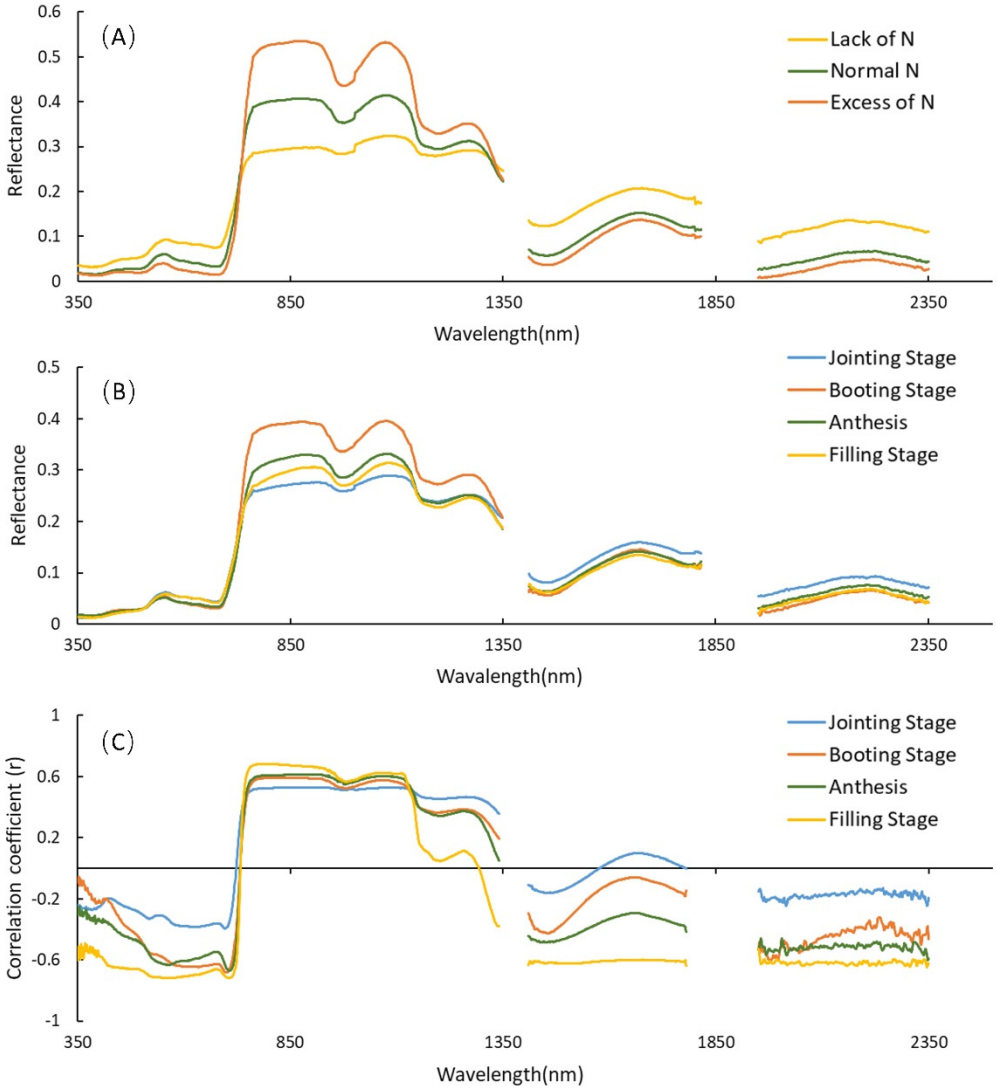

Figure 2. Spectral reflectance properties of the wheat canopy: (**A**) spectral reflectance under N stress; (**B**) spectral reflectance at different growth stages under normal N; and (**C**) correlation between leaf nitrogen concentration (LNC) and spectral reflectance at different growth stages.

During N deficiency, the VIS reflectance of the crop canopy spectrum increased, while the NIR reflectance and red-edge position (REP) decreased; in excess of N, the VIS reflectance decreased, while the NIR reflectance and REP increased (Figure 2) [14,32–34]. As the growth stages proceed, the response of canopy spectral reflectance to crop N status reduced, and the VIS regions also displayed "red shift" and "blue shift" with the development [33,35,36]. It can be found that the analysis of crop N abundance and deficiency using spectral techniques can be specific to a band interval [7,37]. Hyperspectral techniques can even be precise to a specific band [38,39], which provides the possibility of effective identification of crop N deficiency.

The top leaves of the plant under N stress will use the N transferred from the bottom leaves, causing the bottom leaves to yellow and decline prematurely, while the top leaves color changes are not obvious because of being less stressed by N [40,41]. As influenced by the level of soil N supply, the spectral reflectance of leaves at different leaf positions differed erratically in VIS and SWIR, while showing a clear gradient in NIR [42]. Duan et al. [43] suggested that N concentration at different leaf positions decreases from top to bottom at the jointing stage, flowering stages, and filling stage, while the flag leaf stage shows an increasing and then decreasing trend. The vertical distribution of N in the plant is not

constant and varies between N conditions, planting densities and growth stages [41,43,44]. Exploring the spectral response properties of the different leaf positions can serve as a foundation for precise N quantification.

3. Techniques for Remote Sensing Monitoring of Canopy N

The continuous development of remote sensing technology on ground-based, UAV-based, and satellite-based platforms provides a wide range of modal options for N status monitoring studies. There is the technical focus in the field of N monitoring, including exploring the correlations between remotely sensed information extracted from multi-source data and N status, while achieving accurate modeling inversion of N status. To summarize the relevant technologies, three main aspects are discussed: remote sensing monitoring platforms; the correlation between remotely sensed data and N status; and the retrieval methods of canopy N status.

3.1. Remote Sensing Platforms for Canopy N Monitoring

3.1.1. Ground-Based Platform

Spectral data collected by ground-based sensors can be divided into non-imaging spectral data and imaging spectral data, with a spectral range primarily in the VIS–NIR, and in several studies involving the SWIR [18,45]. This close-range spectral information has ultra-high spectral resolution and can respond to subtle changes in N. It has been widely used in N monitoring for both leaf and canopy scale. Non-imaging spectral data are point spectral data, and lack spatial information for N estimation at regional scale [46]. Imaging spectral data, on the other hand, combine spatial and spectral features and allow the estimation of canopy parameters from faceted data. However, due to being restricted by data volume and acquisition method, it is generally used for ground study and rarely used directly for diagnosis and applications of large area. Current ground-based spectrometers used commonly include ASD FieldSpec (Analytical Spectral Devices, Boulder, CO, USA), RS-5400 (Spectral Evolution, Haverhill, MA, USA), HR-1024i (Spectra Vista Corporation, Poughkeepsie, NY, USA), SOC710 (Surface Optics Co. Ltd., San Diego, CA, USA), and FISS (Institute of Remote Sensing and Digital Earth, Chinese Academy of Sciences, Beijing, China) [47–50], etc. These instruments provide a stable and high spectral resolution, but some of them are heavy and are generally measured in a backpack or mounted on a tripod in research, with a single angle and way of acquiring data. The advent of hand-held instruments such as the RapidSCAN (Holland Scientific Inc., Lincoln, NE, USA), 4300 Handheld FTIR (Agilent Technologies Inc., Santa Clara, CA, USA), and Crop Sense (Beijing Academy of Agriculture and Forestry Sciences, China) [51,52] symbolizes the development of spectral sensors towards lightweight and flexibility. The portable spectrometer can acquire data on a wide range of measurement scales flexibly and efficiently, and it is easy to install on a variety of platforms such as lab benches, black boxes, and rocker arms. In addition, the multi-angle spectral acquisition device [53–55] consists of several moving parts to adjust the observation position and direction, where a goniometer is often used to control the observation of zenith angle changes. The sensor is placed on the goniometer to obtain spectral data in the viewing zenith angles (VZA) ranged from -60° to 60° [53,54]. It is a convenient platform for obtaining multi-angle crop spectral data, which has many applications in the study of the vertical distribution of N in the plant canopy.

3.1.2. UAV-Based Platform

With the development of lighter and smaller sensors and the increased carrying capacity of UAVs, the UAVs carrying sensors for data acquisition have become mainstream platforms in crop N monitoring. It is possible to rapidly acquire ground data with high spatial, temporal, and spectral resolution, facilitating the research at small and medium scales. Compared to airborne platforms (operating at kilometers of altitude), UAVs have the benefit of low cost, low operating altitude, and greater flexibility in terms of data collection arrangements. The sensors currently on UAVs specifically include digital cameras,

multispectral/hyperspectral sensors, infrared thermal imagers, chlorophyll fluorescence sensors and LIDAR sensors [56–61]. The hyperspectral imaging spectrometer perfectly combines the advantages of spectroscopic and imaging technology for use in a large area. The payload of UAVs has made lightweight, low-cost sensors a research focus, and airborne hyperspectral imaging spectrometers such as the UHD185-Firefly and Cubert S185 (Cubert GmbH, Ulm, Baden-Württemberg, Germany), and Micro-Hyperspec (Headwall Photonics Inc., Boston, MA, USA) [62–64] are already being used for N monitoring. The PIS112 hyperspectral imaging spectrometer (Beijing Academy of Agriculture and Forestry Sciences, China), GaiaSky-mini hyperspectral imaging camera (Sichuan Dualix Spectral Imaging Technology Co., Ltd., Chengdu, China) [65] and other sensors, as well as the eight-rotor unmanned aircraft system based on RGB and 25-band small multispectral cameras (Zhejiang University, China) [66,67] developed by multiple teams in China, have also been used for agricultural monitoring with good results. Among the image data acquired by the UAV platform, hyperspectral can show subtle changes in crop spectral reflectance features due to its narrow bandwidth and wide continuous spectral range, which is conducive to the fine monitoring of crop N. Most of the multispectral data are small in volume and the spectral range encompasses the N response sensitive VIS–NIR bands. However, the low spectral resolution tends to result in "missing" spectral information while overcoming the high redundancy of hyperspectral information. Studies using multispectral data sources must consider whether the 'missing' spectral information contains sensitive bands and how it can be modeled. UAV remote sensing is not affected by the external environment, such as the atmosphere, and provides better access to high-quality spectral information, making it a common data source for crop N research.

3.1.3. Satellite-Based Platform

Images acquired by satellite platform sensors are characterized by a large range and multiple time phases, making large-scale spatial monitoring possible. Satellite data commonly used for agricultural monitoring include Landsat, Sentinel-2, etc. [68–71]. The small canopy area of rice and wheat requires high temporal and spatial resolution of data in seasonal N management. RapidEye, WorldView-2, etc. have better results in terms of temporal and spatial resolution, and the indices constructed in this way have achieved better results in N monitoring [72–74]. It is of practical significance to monitor crop N in large areas by satellite remote sensing with high spatial and temporal resolution. However, the use of field canopy spectral reflectance to simulate the spectral bands of satellite multispectral sensors, and then transfer the N response models from field experiments to satellite images, inherently results in mistakes due to the low spectral resolution of the data [75,76]. Since the 20th century, China has launched a series of resources satellites, HJ-1A/1B satellites and GaoFen (GF) satellites, etc. [77–81]. The types of sensors and spatial resolution they carry have reached international advanced levels, and their applications in agriculture are gradually spreading. Among them, GaoFen-6 (GF-6) is the first GF satellite for precise agricultural monitoring, for the first time adding green vegetation-sensitive red edge spectral bands and operating in a network with GaoFen-1 (GF-1) to significantly improve the monitoring capability of agricultural resources. GF-6 has been shown to be effective in improving the accuracy of image classification [78–81], and research into the quantitative inversion of crop parameters is still in its infancy. Satellite imagery has a high point and a wide field of view, but the quality has uncontrollable factors. Acquisition is influenced by radiation, aerosols, and weather, increasing the image processing process; analysis is influenced by complex geography and the presence of mixed image elements, increasing the difficulty of N estimation. The effectiveness of crop N estimation models based on satellite imagery still needs to be improved. In addition, as some important reflectance features associated with N can only be measured by hyperspectral sensors, future research could be explored based on satellite hyperspectral imagery.

Remote sensing technologies from ground-based, UAV-based, and satellite-based platforms are maturing and have been widely used in agriculture (Figure 3). The different

platforms have their own advantages in remote sensing monitoring, with their mounted sensors having a high degree of overlap in the wavebands sensitive to N (Figure 4). Crop N monitoring based on ground-based and UAV-based platforms has been effective. Because these platforms provide highly accurate data, more valid information can be mined from spectroscopy, graphics, etc. Satellite data, although limited by data volume and accuracy, has become an effective complement to them in expanding the scale of research. Research on multi-sensor and multi-platform joint observations is gradually being developed.

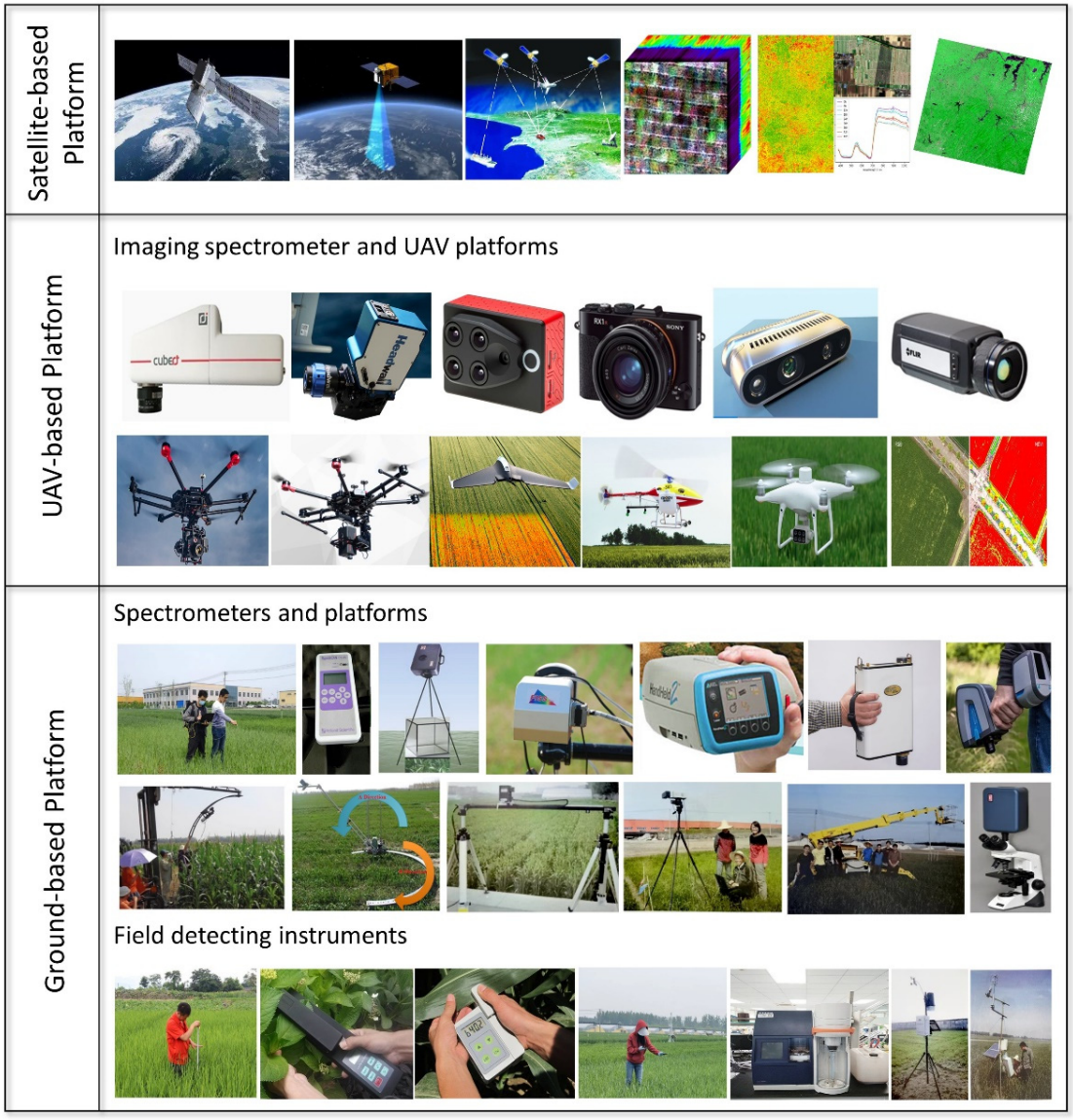

Figure 3. Remote sensing platforms, including ground-based platform, UAV-based platform, and satellite-based platform.

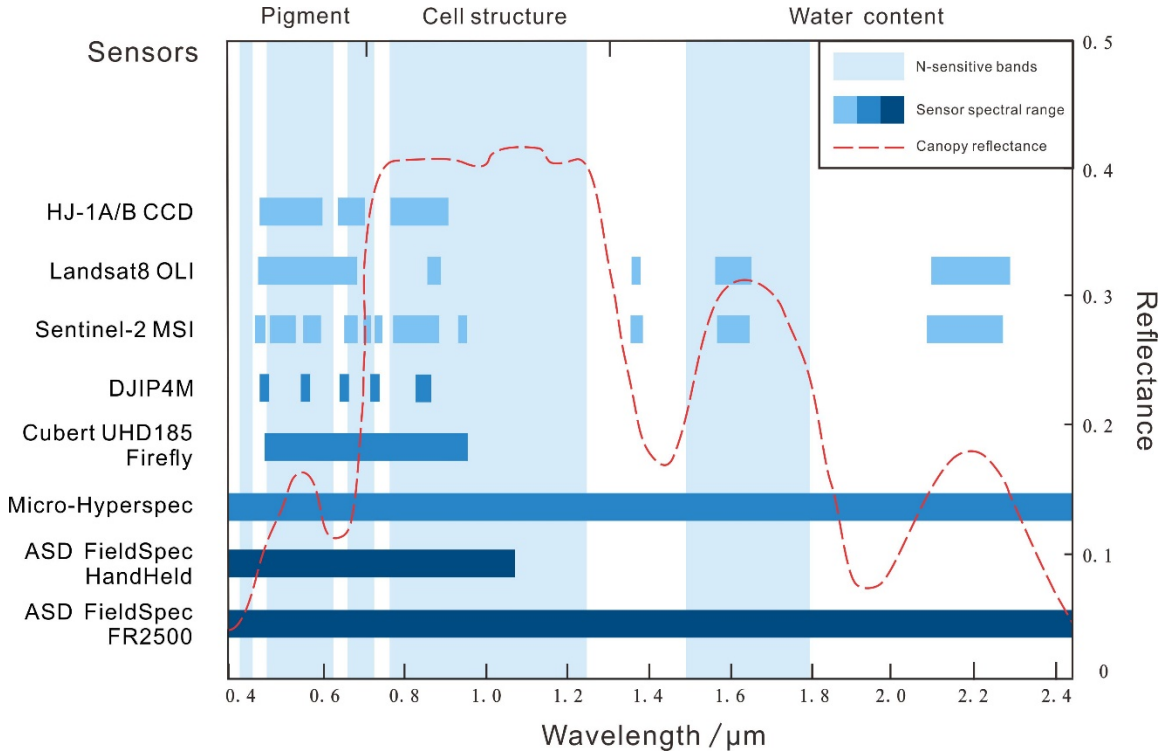

Figure 4. Spectral reflectance properties of crop canopy and spectral range of different platform sensors.

3.2. Correlations between Remotely Sensed Data and N Status

Crop N status can be distinguished between two measurement perspectives: one is area-based measure "nitrogen content" (N_{area}, per unit area); another is mass-based measure "nitrogen concentration" (N%, per unit dry matter) [28]. N% can be converted to N_{area} by plant leaf (or other plant organs) dry biomass. In research, N content generally includes leaf/plant nitrogen accumulation per unit soil area (LNA/PNA), etc.; N concentration generally includes LNC, plant nitrogen concentration on a leaf dry weight basis (PNC), canopy N concentration (CNC), canopy N density (CND), etc. [28,82]. On this basis, Nitrogen Nutrition Index (NNI) is defined as the ratio of the actual crop N concentration to the critical N concentration. It is a direct indicator of whether the crop N concentration is at an optimum level [83,84]. In existing studies, the accuracy of remote sensing estimates of N content is significantly higher than that of N concentration, due to the fact that N concentration is more difficult to extract from remote sensing information compared to N content [64,85,86]. However, N concentration is not disturbed by density and is more accurate in responding to crop N status [82]. Throughout the whole growth stage of rice and wheat, N concentration has a narrower range of variation with a decreasing trend, and the change rate decreased before it increased; N content is a product of the combination of N concentration and plant dry biomass, so N content has a wider range of variation with an increasing trend [87,88]. With the support of remote sensing technology, the study directly links N indicators and spectral reflectance.

3.2.1. Sensitive Spectral Extraction

Spectral response under crop N stress varies significantly, and the analysis of original hyperspectral information is an intuitive study in N remote sensing assessment [39,89], but the sensitive bands extracted vary for the same/different crops in different geographical environments [90,91]. As in different studies, the N-sensitive spectral bands of rice include 738 nm, 1362 nm, 1835 nm and 1859 nm [90], and also include NIR (>760 nm), visible (355, 420, 524–534, 583 and 687 nm) and red edge (707 nm) region [39]; the N-sensitive

spectral bands of wheat include 440 nm and 610 nm [91], and also include 790.4 nm [92]. Wang et al. [38] explored the best common central bands 822 and 738 nm for LNA estimation in rice and wheat, which can effectively assess the N nutrient status of plants and reasonably reflect the intrinsic N information in different crops. Most studies have extracted several N sensitive bands to estimate crop N by individual spectra or combinations. Although the method is simple, the accuracy is affected by the stability of the spectral information.

Hyperspectral data have hundreds of high-resolution continuous spectral information. When exploring correlations between spectra and N status, using full band data as an input can increase errors and reduce efficiency. Whereas insufficient exploitation and use will lead to data waste, thus losing the significance of high-precision data. Therefore, improving the use efficiency of hyperspectral data still needs to be further explored. Wang et al. [93] divided the spectral data into five groups: blue, green, red, red edge and NIR, and extracted the corresponding N-sensitive bands, in which the red edge (702, 703 and 710 nm) and red edge (706, 733 and 759 nm) correlated with leaf and canopy-scale N status up to 0.92. Yu et al. [94] reduced the spectral data by a discrete wavelet multi-scale decomposition method (DWMD), achieving better results compared to iteratively retaining informative variables, with 16.28–26.23% improvement in coefficient of determination (R^2). Hyperspectral data are very similar between adjacent bands, and their dimensionality reduction can help reduce the complexity of feature extraction. Liu et al. [95] demonstrated that using feature bands extracted by improved adaptive ant colony optimization algorithm as input parameters under the same prediction model can reduce the complexity of the model, while improving the prediction capability. In addition, the autocorrelation matrix (R^2 = 0.86 between N-sensitive bands and N status), the non-negative matrix factorization (R^2 = 0.83), the successive projections algorithm (R^2 = 0.66), and the competitive adaptive reweighted sampling (R^2 = 0.93), etc. are also gradually applied [62,94,96–99]. Improvements to the N-sensitive band extraction method have resulted in the stability of the retrieval N information, but make the processing process more complicated, with a corresponding increase in model performance and computation time [97]. In addition, the bands extracted by these algorithms integrate more reflectance information, which improves stability and anti-interference. This provides a guideline for constructing a unified and generalizable spectral feature extraction method.

3.2.2. Mathematical Transformations of Spectra

The difference in response to N between spectra can be increased by mathematical transformations of spectra, improving its adaptability to inversion N status. The spectral reflectance curve feature can reflect the N change trend, and the first-order derivative of the spectrum indicates the rate of change in the reflectance, which reduces the effect of background information and is widely used in N estimation [63,92,93]. The morphological differences in crop spectra can be described by characteristic parameters such as slope, angle, and rate of change in the curve. Slope and angle are generally calculated based on areas of reflectance that change abruptly, such as peaks and valleys. The slope indicates the rate of reflectance rise/fall, and the angle formed by the sides of the reflection peak and absorption valley indicates the width between the peak and valley [100]. The rate of change is a generalization of the first-order derivative, which can respond not only to the change in reflectance between successive wavelengths, but also to the rate of change in reflectance between any two wavelengths [101]. Based on two integration metrics, normalized area reflectivity curve and reflectivity integration index, Du et al. [58] combined more wavelengths with improved LNC retrieval performance.

The study showed that the red edge region of 700–780 nm is a sensitive band for responding to the growth status of green crops [102,103], and the characteristic parameters of REP, red-edge slope, red-edge peak, red-edge minimum amplitude and red-edge area obtained by mathematical transformation of the red edge band have also become common parameters for N diagnosis in rice and wheat [36,104,105]. The REP based on linear extrapolation method showed better canopy N concentration correlation at larger canopy

cover. Since the first-order derivative has "bimodal" characteristics in the two main spectral regions, the conventional REP is not sensitive enough to canopy LNC only using single-peak maximum, and the spectral reflectance data can be fitted to generate continuous REP values to achieve a continuous relationship between REP and N [105]. Li et al. [106] proposed a continuous wavelet transform-based REP extraction technique, wavelet-based red edge position (WREP), which provides a new idea for understanding the spectral variation in red edge region. Guo et al. [107] constructed an algorithm based on the analysis of red edge features, shifting red edge absorption area (sREA), which enables the construction of N absorption models at the regional scale. Due to the possible discontinuity of changes, insignificant amplitude, and large errors in the RE first-order derivative spectra, the estimation of crop N by red edge parameter features is highly dependent on the feature extraction method. It is necessary to select the appropriate method and parameters according to the research needs. When the canopy cover is too high, the response of the red edge region to N becomes gradually slower and then there is saturation, so only using red edge parameters easily causes misjudgment.

The mathematical transformation of spectra can respond to the trend of N changes, but the spectral information is changed by the influence of environmental stress. Deeply mining the bands with more effective information and using them in combination is the key to overcome the external factors and improve the accuracy of the model.

3.2.3. Spectral Indices

The information presented by specific parameter combinations (mainly difference, ratio and normalized values) is more stable and representative, and it has become the first choice for remote sensing inversion of crop parameters. The development of spectroscopy has improved the accuracy of spectral information, and the methods of first-order derivative, continuum removal, wavelet transform and smoothing algorithm (such as Savitzky-Golay smoothing), etc. are applied to the original spectra, which make the spectral calculation more refined and the results more accurate [95,108,109]. Compared with traditional vegetation indices (VIs), the construction parameters of spectral indices are no longer limited to band reflectance, but can also be red edge parameters, other spectral indices, etc. (Table 1) [26,110,111].

For multispectral/hyperspectral remote sensing data, spectral indices are usually constructed by selecting appropriate bands in the visible red region and NIR region. For different varieties of crops, there are significant differences in the slopes of normalized difference vegetation index (NDVI)-based LNC models, and it is difficult to achieve uniform regression analysis across different crops varieties with conventional indices. It has been shown that $NDVI_{(1220, 610)}$ is a good index to estimate LNC in both rice and wheat, with RMSE all less than 13.04% [34], and $NDVI_{(1220, 710)}$ achieves high precision estimation of N status for different varieties of rice [112]. However, the model has not been extended to other regions for validation, and the accuracy and stability of the spectral index remains to be explored. In addition, the use of a multi-band vegetation index for LNC monitoring in rice and wheat is more effective [92,113,114]. Wang et al. [113] used a three-band vegetation index combining NIR, red edge and blue bands to estimate LNC for rice and wheat with R^2 of 0.866 and 0.883, respectively, which were 17.66% (rice) and 7.68% (wheat) more accurate than NDVI, and 40.13% (rice) and 16.18% (wheat) more accurate than RVI. Tan et al. [92] explored the relationship between LNA and parameters such as first-order derivative sum (SD), first-order derivative maximum (D), etc. in VIS and red edge regions, and the new normalized index $(SD_r - SD_b)/(SD_r + SD_b)$, which was constructed by integrating information from multiple bands, was a good fit for wheat LNA (R^2 = 0.935) and was applicable to wheat N inversion in different varieties and regions.

The N estimation model used fixed VIs performed consistently over the same growth stage, but when pooling data from multiple growth stages, accuracy decreased significantly. Canopy structure and background conditions changed as the growth stage progressed, but in all cases, whole leaf pixels showed more stable performance than light and shade leaf

pixels [87,115,116]. Traditional spectral indices cannot fully capture the intrinsic relationship between canopy spectra and N in growth stage, and how the predicted intensity of N models varies across growth stages has not been fully explored [117]. The red edge chlorophyll index ($CI_{red\ edge}$) is sensitive to canopy N content and can effectively mitigate the effect of canopy structure on canopy N estimation. Li et al. [118] combined NDVI and $CI_{red\ edge}$ to construct a nitrogen planar domain index (NPDI) with good predictive ability for canopy N uptake in wheat, corn and both combinations. Palka et al. [119] constructed a regression model by combining the canopy chlorophyll content index (CCCI) and the canopy nitrogen index (CNI), and modified the CCCI-CNI to extend N estimation to the end of booting stage for wheat. Quantifying the spectral contribution in the mixed image elements using spectral mixture analysis (SMA) can improve the spectral accuracy, and the spectral indices constructed in this way show superior capability in all growth stages and even in the early evaluation of LNC [116,120]. The selection of sensitive multi-band and multi-index information fused to form a spectral index improves the sensitivity of N inversion, and to some extent overcomes the inconsistency between indices and N for different varieties of crops and different fertility stages.

Based on RGB data, the response of different image indices to N varies widely and has limited response [121]. The RGB three-color channels of UAV images each contain luminance information and are susceptible to interference from lighting conditions. In contrast, in the HSV and Lab color spaces, V and L denote value and luminosity, respectively, and the transformation of RGB to them weakens the influence of luminance information through nonlinear changes, resulting in a more sensitive response to LNC [122]. Nevertheless, RGB is limited by spectral accuracy and still has difficulties in index improvement. In addition to the color information extracted from spectral data, the texture information can be obtained from the local variance function, which reflects the variation relationship between several pixel points and characterizes the canopy structure. Fusing two or more datasets with different feature information can provide a more comprehensive interpretation of the relationship between remote sensing information and N status [123]. Therefore, for RGB data, the "image-spectrum" fusion indices formed by fusing image indices and texture features improves the sensitivity of image data to N features, and the investigation of its ability to diagnose N status is a major development direction at present [60,82]. When extracting texture features through Gray-level Co-occurrence Matrix (GLCM), crop cultivation patterns may cause differences in texture information metrics for N content in different directions, and using texture information calculated along the perpendicular to the row direction to monitor row-grown crops has the best results [85]. In addition, adding depth information to RGB images can break through the limitations of extracting canopy structural features from 2D images [86,124]. Xu et al. [124] fused texture features with 3D structural information and RVI to invert N status with better accuracy and stability, the LNA prediction accuracy of 0.74 during whole growth stages. By adding 2D and 3D structural information, the background and saturation effects can be better reduced, and the N inversion information of the crop canopy can be enhanced.

3.3. Retrieval Methods of Canopy N Status

For crop N status assessment and monitoring, the modeling methods can be divided into statistical analysis, physical analysis, and hybrid methods. Statistical analysis is to obtain high-precision N diagnosis by establishing mathematical relationships between ground truth data and remote sensing spectral information, which can be further classified into two categories: traditional statistical methods and machine learning methods. Physically based methods take the structural information and physicochemical properties of plants and leaves as input parameters, simulate the process of radiation absorption and scattering inside the crop, and form the reflection spectrum and output, so as to establish the correlation between crop parameters and ground reflection spectrum. The models are divided into radiative transfer models (RTM) and geometric optical models, and RTM are often used in research because of the continuous and uniform distribution of rice and wheat

in cultivation. Hybrid models have advantages by using multiple categories of models in combination but are currently used rarely in N retrieval (discussed in Section 5).

Table 1. Spectral indices for assessing crop N status.

Index	Formula	Reference
Nitrogen Reflectance Index	$\frac{(R_{800}/R_{550})_{target}}{(R_{800}/R_{500})_{reference}}$	[125]
Red Edge Position: Linear Extrapolation Method	linear extrapolation of two straight lines on the derivative spectral curve (lines formed by 680 nm and 694 nm, and formed by 732 nm and 760 nm)	[126]
Normalized Difference Red Edge	$\frac{R_{790}-R_{720}}{R_{790}+R_{720}}$	[33]
Double-peak Canopy Nitrogen Index	$\frac{(R_{720}-R_{700})/(R_{700}-R_{670})}{R_{720}-R_{670}+0.03}$	[127]
Nitrogen Planar Domain Index	$\frac{Measured\ CI_{red\ edge}-CI_{red\ edge}\_MIN}{CI_{red\ edge}\_MAX-CI_{red\ egde}\_MIN}$	[118]
Water Resistance Nitrogen Index	$\frac{(R_{735}-R_{720})R_{900}}{R(R_{930}-R_{980})(R_{735}+R_{720})_{min}}$	[128]
Canopy Chlorophyll Content Index	$\frac{NDRE-NDRE_{\min}}{NDRE_{max}-NDRE_{\min}}$	[129]
Modified Chlorophyll Absorption Ratio Index	$\frac{R_{700}-R_{670}-0.2(R_{700}-R_{550})}{R_{700}/R_{670}}$	[130]
MCARI/MTVI2	$\mathrm{MCARI}=\frac{R_{700}-R_{670}-0.2(R_{700}-R_{550})}{R_{700}/R_{670}}$ $\mathrm{MTVI2}=\frac{1.5(1.2(R_{800}-R_{550})-2.5(R_{670}-R_{550}))}{sqrt\left((2R_{800}+1)^2-(6R_{800}-5sqrt(R_{670}))-0.5\right)}$	[131]

R_i stands for reflectance at wavelength i nm.

3.3.1. Traditional Statistical Methods

Traditional statistical methods have simple mechanisms, and their inverse accuracy depends more on the rationality of modeling parameters, thus they cannot overcome the influence of environmental and other factors, and there are difficulties in transferring prediction models to other datasets. However, due to the simplicity and convenience of the model and its usability, it is still widely used in the field of crop N monitoring at present. Univariate linear regression and its nonlinear transformation, as the basis of statistics, have achieved good results in exploring whether there is a significant correlation between crop N indicators and individual VIs, and occupy an important position in N status inversion [104,132,133]. Hansen et al. [89] found that applying partial least squares regression (PLSR) to fit N status gave equal and better results than exponential regression, with the R^2 maximum increase of 23%. PLSR was considered a good alternative to univariate statistical models. When multiple growth stages are involved or when there is a lack of phenological information, individual index that do not fully utilize spectral data cannot describe the relationship between N and spectral information, so using multiple linear regression (MLR) is a better choice [134]. MLR can reduce model chance. Whether the parameters involved in modeling exist in response to N and whether there is overfitting between parameters is the key to influencing the multiple regression model. Pearson correlation coefficient is generally used as a measure in the study, and the combination of parameters with larger correlation coefficients is selected to construct MLR models with good interannual scalability [64,69]. PLSR, principal component analysis (PCA), stepwise multiple linear regression (SMLR), and Ridge Regression, etc., play an advantage in dealing with the collinearity problem between parameters. Many co-linear spectral variables were reduced to a few uncorrelated latent variables to avoid overfitting problems [91,123,135]. The selection of a suitable variable dimensionality reduction method based on the quantitative relationship between the number of samples and the dimensionality of variables, combined with multiple regression, significantly improves the inversion accuracy and applicability.

Traditional statistical methods can describe different rates of change between N status and spectral information, providing fitting models for a variety of change conditions. For region-specific datasets, models with good inversion effects can be obtained by comparing different regression methods; for datasets with different growing environments, the best regression models derived from the study will be different [64,89,104,134]. Although the statistical models are not stable enough to overcome environmental problems, the different regression methods in the statistical models are more consistent in principle, have specific mathematical relationships, are easy to understand and apply, and are extremely convenient to use in fixed research areas. Therefore, the traditional statistical methods still dominate the existing N remote sensing monitoring studies.

3.3.2. Machine Learning Methods

Machine learning models are gaining widespread attention for their ability to handle large amounts of input data from multiple platforms and to solve nonlinear tasks. Artificial Neural Network (ANN) and Back Propagation Neural Network (BPNN) are commonly used models for remote sensing estimation of crop N status, which can automatically extract relevant features from data. However, in practical applications, a large training dataset is required, and the number and size of the implied layers, training efficiency, and overfitting are considered. Yang et al. [96] used Gaussian radial basis function as the implied layer of the neural network to avoid the tedious calculation and overfitting phenomenon of BPNN, with structural adaptive features, good generalization ability and fast learning convergence speed, and more stable and reliable application. When constructing neural network models directly, the differences in results for different types of parameters are not obvious, but the accuracy is significantly improved after using PCA for model input parameters [136–139]. The combined use of PCA and machine learning methods shows unique advantages and promising applications.

Support Vector Machine (SVM) is extremely effective for analytically solving high-dimensional data problems. Yao et al. [140] applied traditional regression analysis, ANN and SVM, to compare the prediction accuracy, computational efficiency and complexity level of different methods for inversion of wheat LNC. The results showed that the machine learning models were more accurate, with the SVM method being more stable in dealing with potential confounding factors for most varieties, ecological niches, and growth stages. The kernel function in SVM is the focus of attention, and the multiple-kernel support vector regression (MK-SVR) plays an advantage in estimating N status at different growth stages because it combines the advantages of local kernel function and global kernel function [141]. However, complex optimization algorithms can reduce the computational efficiency of SVM and using a combination of least squares and SVM methods, LS-SVM can solve linear or nonlinear multivariate estimation capability in a relatively fast way, significantly improving the computational efficiency of SVM [17,141,142].

In the presence of weak a priori knowledge, Gaussian Processes Regression (GPR) can perform adaptive nonlinear fitting of complex datasets with flexible probabilistic Bayesian models and simpler parameter optimization applied to crop N status inversion [11,93,143]. Random Forest (RF) integrated with decision trees as the basic unit can rank the importance of variables, reduce redundancy in high-dimensional datasets, and have high stability, with vast application prospects [37,144]. When the entire spectral range of a single band is used as an input variable, the accuracy of regression by RF inversion (R^2 = 0.89) is higher than that of univariate regression with existing VIs; when VIs is used as input features, model accuracy is improved with R^2 of 0.95 [145]. Determining the appropriate input dataset is a key element to exploit the predictive power of the model.

Machine learning methods techniques can be used to reveal the physiological and structural characteristics of plants, and can respond to dynamic differences in physiology due to environmental influences [144]. The study is no longer limited to conventional machine learning models, but improves the models starting from input datasets [138,145], model parameters [96,144], functions and structures [17,96,141], which not only improves

the efficiency of data analysis, but also enables higher accuracy N status analysis, making it more efficient and flexible in N monitoring. The input variables have diversified from single spectral information to mathematically transformed spectral data, spectral indices, and texture information, etc. while the machine learning methods are expanding toward efficiency, accuracy, and speed.

3.3.3. Physically Based Methods

RTM use optimization algorithms for inversion to infer the N content of crops from observed spectral data. Depending on the scale of the object of study, it is mainly divided into leaf radiative transfer models and canopy models. At the leaf scale, the PROSPECT model is the most widely used and has been continuously optimized and improved [146–148]; at the canopy scale, the SAIL model is one of the first models applied, mainly for uniformly distributed continuous vegetation surfaces [149]. Combining PROSPECT and SAIL models to invert vegetation physiological and biochemical parameters is a common approach nowadays, mostly around canopy and LCC, water content and leaf area [29,75,150,151]. Most studies derive crop N status through empirical relationships based on significant associations between leaf area or Chl and N. Despite the long-standing stability and reliability of RTM in the inversion of physicochemical parameters, different configurations of the model by users may lead to equally plausible results [152,153], so it is necessary to constrain the model using a priori information. Combining the DSSAT cropping system model CSM and PROSAIL model, complementing the interaction between crop growth stages and the environment for the constraints of the input parameters of the PROSAIL model, plays a unique advantage in the inversion of crop physicochemical parameters, not only with high accuracy, but also with the statistics of physicochemical parameters among different varieties of crops [154].

Yang et al. [155] used N uptake coefficients to equivalently replace the Chl uptake coefficients in the original PROSPECT model, and established the N-PROSPECT model based on the PROSPECT model to directly invert leaf N content. The N-PROSAIL model, established by combining the N-PROSPECT model and the SAIL model, achieves the diagnosis of N status at the leaf and canopy scales, and reduces the model error by setting a priori parameters at different growth stages [156]. The RTM expresses the crop growth process from a physical point of view, which is more stable in the inversion, but has the problem of being time-consuming. Combined with the Lookup Table (LUT) it can reduce the computational demand. Li et al. [157] constructed a multi-LUT for wheat LAI, LND and two spectral indices (MSR and MCARI/MTVI2), which not only reduced the LUT size and improved the computation time, but also had better accuracy of N estimation. On the other hand, since protein is also a major N-containing component in crops, coupling protein specific absorption coefficients into the PROSPECT model to form PROSPECT-PRO, which is combined with the 4SAIL model to form PROSAIL-PRO, can also be used for crop N status diagnosis [31,158]. RTM with strong explanations is better expressed in the inversion, but because the model expression depends on the input of more parameters and complex computational process they are less used in current research. Reducing the complexity of models and complementing the advantages of statistical models, hybrid RTM and machine learning models have become a future research need.

4. Influential Factors on Accuracy of Remote Sensing Monitoring of Canopy N

Spectral reflectance information has been shown to be sensitive to the N content of canopy leaves, but differences in data acquisition, vertical distribution of leaf N, dynamic changes in N during the growth stages, and physiological differences between different plants can all have an impact on the correlation between crop spectral information and canopy N indicators.

4.1. Differences in Data Acquisition Angles

Both portable spectrometers and UAV sensors usually acquire spectral data for crop N monitoring within a range of VZAs, which can vary by 30° and more. The spectral indices in crop N status studies are usually developed from vertical angle data. However, due to the variation in the angle of view of data acquisition caused by different experimental conditions, and the anisotropy of vegetation reflectance, the accuracy and robustness of using these indices directly to estimate the N content are not sufficient. The reflectance in the VIS, red edge and NIR bands decreases gradually from VZAs from −60° to 0°, with relative changes in reflectance ranging from 34.7% (+60°) to 265.5% (−60°), and 81.7% (+60°) to 89.3% (−60°) in the VIS and NIR bands, respectively [53]. Therefore, developing an index that is sensitive to N content and insensitive to VZAs is of great practical importance to adapt to different experimental conditions, improve prediction accuracy and enhance model stability.

Higher viewing angles allow better extraction of crop biochemical information compared to the nadir orientation [159]. The change in view angle significantly affects canopy reflectance, especially in the red and NIR bands, which in turn makes VIs based on these spectral bands sensitive to angle [160]. The introduction of angle-insensitive bands to construct indices, such as the normalized difference red edge (NDRE), the green and blue bands, and the green band Chlorophyll Index (CIgreen), can improve the accuracy of canopy N inversion of different VZAs remote sensing images, significantly expanding the range of suitable viewing angles for determining crop N status by remote sensing, and thus adapting to the differences between different experimental conditions [53,161,162]. For the angular insensitivity index cannot be simply attributed to the effect of a single band; green, blue and NIR bands may have played a joint role in improving the index adaptation. It is difficult to obtain accurate spectral collection perspectives in the applications. A unified N monitoring model under a range of perspectives can help with the flexible application of crop N diagnosis. Like other VIs, Li et al. [53] developed angular insensitivity vegetation index (AIVI) to have the best LNC estimation accuracy at −20° view angle, but at the same time the correlation between AIVI and LNC has high stability at −10° to −40° with R^2 of 0.83. Similarly, floating-position water band index (FWBI) has the highest correlation with LNC at −10° view angle (R^2 = 0.852), also has superior N content estimation accuracy at 0° to 30° (R^2 = 0.835) [161]. The statistics on angular differences show that back-scatter direction has better LNC prediction accuracy than the forward-scatter view angle.

However, the spectral information obtained by whatever VZAs inevitably has information such as soil background, light shading, etc. Different growth stages and different light conditions will change the crop spectral reflectance, which is a common noise in inversion. The study reduces their effects by spectral preprocessing such as first-order differentiation and wavelet transform, suitable vegetation index, and threshold segmentation [27,63,82,93]. The water background of rice is a unique feature that differs from other crops; water has an absorption effect on the NIR band, and when the canopy cover is small, the water depth and turbidity have an isotropic effect on the spectral reflectance of the red-edge region [163]. Therefore, when converting reflectance to vegetation index, this effect can be eliminated or attenuated by calculating between multiple bands. The individual N content was significantly improved in accuracy before and after removal, and the group indicators indicated the total amount per unit area, which was less influenced by background noise and had a smaller enhancement effect [82].

4.2. Vertical Distribution of Leaf N

When the canopy leaves are taken as a whole object, most of the studies are carried out for the upper leaves, ignoring the vertical heterogeneity of the canopy. The LNC within the canopy is not constant from the top to the bottom of the leaf layer, and it varies with growth stages. At jointing stage, flowering stage and filling stage, LNC decreases from top to bottom; and at booting stage, it tends to increase and then decrease [43]. Moreover, it is difficult to effectively identify the information at the bottom of the canopy by acquiring

the crop reflectance spectra vertically due to the influence of canopy leaf cover at different growth stages. At present, we have achieved better results in exploring the canopy N content by acquiring reflectance spectrum vertically or from multiple angles to overcome the stratification differences.

The PLS algorithm has better estimation capability for different levels of leaf N status, then becomes an effective tool for early N monitoring [40,164–166]. Huang et al. [164] combine NRI and NPCI to construct a PLSR model which could better retrieve foliage N density in different leaf layers ($R^2 > 0.67$). He et al. [166] also demonstrated that PLSR estimates LNC accuracy better than BPNN and eXtreme gradient boost (XGBoost). However, for the studied spectral information, which must contain information from different leaf layers, it is especially important to determine the contribution of different leaf layers to the spectral reflectance of the canopy. Studies have begun to explore the characteristics of the vertical distribution of N in the canopy of crops at different growth stages, and to develop an effective method for estimating N in each leaf layer or total N in the canopy by determining the correlation between different leaf layers and N status [40,43,44]. Duan et al. [43] used a calibration coefficient to adjust the relationship between the effective layer of remote sensing detection and the whole canopy, and then developed a method for estimating the overall canopy LNC based on GI, mND705 and NDVI. He et al. [44] estimated the canopy top LNC by NDRE, then inputting the results into the LNC vertical distribution model to get the model coefficients; thus the model based on the relative canopy height could obtain LNC in different leaf layers (LNC_{Li}), which was superior because of fewer parameters and higher accuracy. The short plant size of rice and wheat crops and the small vertical distance between different leaf layers can easily mask differences in the spectral response of canopy N status changes [54]. Compared with vertical remote sensing observation, multi-angle observation can reduce the information bias of fixed viewpoints. Using different combinations of VZAs, Wu et al. [54] were able to retrieve LCC in the upper-layer (VZA 10°), middle-layer (VZA 10° and 30°) and bottom-layer (VZA 10°, 30° and 50°) of the plant, respectively. Based on the response of spectral indices to each leaf layer of N status at different VZAs, selecting the best VZAs or combination of VZAs can realize the complementation of canopy spectral information so that the accuracy of crop N monitoring can be more robust and accurate [40,54].

Multi-angle stereoscopic observation can obtain more vertical information about the plant, but when the bottom leaves are too low, the influence of soil background and crop residues, etc., will increase. Therefore, it is necessary to determine the effective depth of crop canopy spectroscopy observation and realize the inversion model of vertical distribution of N content in canopy from "surface" to "three-dimensional". At the same time, the multi-angle measurement will generate a huge amount of data, and how to quickly extract the effective information from it has become an urgent problem to be solved.

4.3. Dynamic Changes in N during the Growth Stages

N content in crops is a long-term accumulation process that changes as growth stages. The correlation between N and spectral information varies at different stages, and an ideal N inversion model needs to overcome the effects of phenological variability and accurately estimate the N content of the crop at different growth stages. Throughout the crop's reproductive stages, temperature levels affect photosynthesis and metabolic processes that are closely related to N assimilation and utilization. Therefore, it is necessary to introduce meteorological information to construct a dynamically changing model.

Crop models such as CERES and APSIM, which are widely used around the world, simulate crop growth processes by inputting meteorological data and field management data, etc., and are important guides for real-time diagnosis of crop N nutrition status under different cropping conditions [167–169]. The construction of growth models relies on numerous experimental parameters, which are data-intensive and cumbersome to process. Cao et al. [170] dynamic obtained relative growing degree days (GDD) based on the physiological development time of crops to participate in modeling, and quantified

the model parameters that reduced the effects brought about by different indicators. In addition, the field spectral information obtained based on remote sensing data is accurate, and quantitative analysis of temporal variation between VIs is more conducive to the dynamic monitoring of N status. Double Logistic functions and Gaussian curves fitted to time-series data can effectively describe crop growth and senescence processes [171–173]. By combining effective accumulated temperature and crop growth parameters, such as the spectral index NDRE, a model for monitoring the entire growing period of the winter wheat canopy, constructed with the growing degree-days as a moderating factor, offers the possibility for N estimation throughout the growth stages [174]. Dynamic curves of indices such as NDVI, constructed using accumulated growing degree days (AGDD) as a time driver, provide a reference for N nutrition diagnosis at different periods [172]. Combining multi-temporal VIs with key phenological indicators, the constructed dynamic model has clear biological significance, which not only facilitates crop N monitoring but also significantly enhances the ability of N status early prediction.

4.4. Physiological Differences in Plants

N synthesis is influenced by canopy structure, photosynthesis-related pigments, and water content, etc., and confounding effects are common in canopy reflectance under physiological stress, making N remote sensing monitoring challenging.

Water is the carrier of N transport in the crop and is closely related to the N status of the canopy. Exploring the spectral response to N and water shows that the spectral reflectance of wheat treated under low water conditions increases in both regions of SWIR, with less difference in the NIR region under water differences [27,59]. Thus, indices constructed based on SWIR and NIR reflectance are better able to show differences between N levels in different water treatment environments. The SWIR region contains more water-related information, but sensors that include SWIR are costly so it is relevant to explore water-sensitive bands in the VIS–NIR range. Under the condition of constant N content, the red edge reflectance of crops with different water treatments tends to be the same [128]. Based on the red-edge correlation indices such as NDRE and normalized pigment chlorophyll index (NPCI), the introduction of water-related indices, such as floating-position water band index (FWBI), crop water stress index (CWSI), etc., can significantly improve the interaction between water deficit and N nutrition [128,175–177]. Whether the multi-analysis based on specific VIs or the whole spectrum, studies have been conducted to separate N and water information in the spectrum by reducing spectral mixing effects, thus improving the estimation accuracy of crop N under the influence of water.

Crop growth parameters are not independent of each other and may correlate under different circumstances, such as correlation between N, Chl and LAI when the canopy cover is small. However, when Chl and LAI change driven by other external conditions, there will be errors in estimating N status based on their correlation with N. Research needs indices that are both sensitive to N and resistant to interference from other factors. The combination of two VIs with different sensitivities to Chl and LAI, whose ratios can minimize the effect of LAI and have a better correlation with Chl, such as the joint indices modified chlorophyll absorption ratio index and second modified triangular vegetation index in ratio (MCARI/MTVI2) [131], the red-edge-chlorophyll absorption index and the triangular vegetation index in ratio (RECAI/TVI) [111], the transformed chlorophyll absorption reflectance index and optimized soil-adjusted vegetation index in ratio (TCARI/OSAVI) [177]. The red edge region is influenced by LAI which cannot estimate N well in complex situations. Chen et al. [127] found that there is a double-peaked phenomenon in the first-order derivative spectrum of the red edge region, and that changes in N concentration can be amplified as changes in the relative height of the double-peaked peaks, with which the proposed double-peaked canopy nitrogen index (DCNI) can overcome the influence of LAI. There is a certain similarity between different spectral indices and different physiological parameters, which show hierarchy and aggregation in statistical analyses. Exploring the different

relationships that may exist between parameters is therefore important for exploring N status in crops grown under different growing conditions.

5. Challenges and Perspectives

After decades of development, the techniques for remote sensing monitoring of canopy N have made rapid progress and achieved good results, but there are inevitably many difficulties and challenges that need to be addressed.

(1) The development of multi-source data integration from "satellite–airborne–ground" to meet the needs of high-precision monitoring at all scales. In recent years, remote sensing-based crop N monitoring and assessment research has been conducted mainly at the laboratory and field scale, applying small sensor platforms based on ground-based spectral instruments and UAV to acquire data. Research on large farms, counties, cities, or larger regional scales rely on satellite-based multispectral data. Multispectral data are affected by radiation and atmosphere during acquisition, making processing more difficult. In the face of complex geography, the low-resolution images are prone to mixed pixels, making it difficult to achieve accurate estimates of N status. Hyperspectral data are limited at large scales due to their access and data volume, so how to achieve high accuracy monitoring and assessment of crop N over large scale areas is a major challenge currently faced.

Currently, the research on crop N estimation from UAV data is beginning to bear fruit, with good validation in small farm applications. A summary of the spectral data acquisition platforms and their inversion N in existing studies is shown in Table 2. UAV-based research can not only analyze spectral information (sensitive spectra, spectral mathematical transformations, spectral combination calculations, etc.), but also extract image information (texture information, color information, etc.), which shows advantages of high precision due to its high spatial and temporal resolution and the amount of representation information. Satellite-based imaging data are limited in depth, mostly only extract VIs result in low inversion accuracy, yet satellite data is still the most important source of data for large-scale studies. In the existing research situation, the rapid development of sensor technology and remote sensing platforms has extended the scale of research to medium and large farm areas. The results of existing UAV-scale research results are translated to municipal, provincial, national, and even larger scales through algorithms such as multi-scale analysis and reconstruction, and spatiotemporal data fusion, thus enabling N monitoring over large areas. Therefore, the fusion of multiple sources of data from "satellite–airborne–ground" is the basis for large scale applications with inversion accuracy [178]. At present, the spectral resolution of the red edge and NIR bands (N-sensitive bands) in satellite-based hyperspectral sensors is insufficient, and the spatial resolution and revisit period are not advantageous. In this context, the transformation of ground-based research results and the development of high-precision satellite-based hyperspectral sensors deserve even more attention. From the perspective of data acquisition, the complementary advantages of the multiple types of data from "satellite–airborne–ground" could break the limits of geographical scope, and then enable high-precision monitoring and assessment of crop N status at all scales.

(2) Research still has bottlenecks in monitoring crop N in the presence of confounding factors. Under N stress, the spectral properties of vegetation leaves change, and N monitoring is achieved through crop spectral information obtained from ground-based observations by remote sensing technology. However, in practical applications, the inconsistency of crop growth conditions can lead to irregular overall crop deficiencies in water, fertilizer, and cause pests and diseases, all of which could generate yellowing and wilting of crop leaves. The changes in the external structure and intrinsic characteristics of the canopy, result in corresponding changes in the spectral reflectance characteristics [178]. To simply attribute spectral changes to canopy N content would be a misjudgment. Studies are generally set up with variable conditions for different growth stages, locations, field management, species, or plant types to test the stability of the model. However, there is insufficient evidence that the method is effective in overcoming spectral variation due to

physiological differences. The primary way to achieve interpretability and practical application of the model is to start with the principles and isolate the influencing factors [179,180]. When considering only N and another stress factor, overcoming the effects of water can increase R^2 to 0.843 [128]. However, few studies have quantified and differentiated the contribution of leaf biochemical content (including water, diseases, other pigments, etc.) to the spectral band from spectral perspective.

Table 2. Summary of the data platforms, retrieval methods, and research results of the studies cited in the body.

Crop	N Status	Data Platforms	Indices	Retrieval Method	Results	References
Wheat	LNA	ASD FieldSpec Pro	Spectral bands VIs	PLSR SVM RF	R^2 = 0.895 RMSE = 0.903 g/m^2	[109]
Rice	LNC CNC	ASD FieldSpec Pro2500 ASD FieldSpec3	Spectral bands VIs	GPR RF, GPR-RF SVR, GPR=SVR	R^2 > 0.94 NRMSE < 6%	[52]
Wheat	CND	ASD FieldSpec Handheld UAV (UHD 185 Firefly)	VIs	N-PROSAIL	Field: R^2 = 0.83 RMSE = 0.23 UAV: R^2 = 0.74 RMSE = 0.26	[157]
Wheat	N concentration N content	ASD FieldSpec HandHeld	Spectral bands VIs	Statistical analysis	N concentration: R^2 = 0.81 RMSE = 0.72% N content: R^2 = 0.96 RMSE = 0.83 g/m^2	[119]
Wheat	LNA	ASD FieldSpec HandHeld 2 RealSense depth camera D435i	VIs Texture	MLR BP	R^2 = 0.74 RRMSEs = 40.13%	[124]
Rice	LNC	UAV (AIRPHEN multispectral camera)	VIs	Linear spectral mixture analysis Statistical analysis	R^2 = 0.78 RMSE = 0.26% RMSE = 10.4%	[116]
Wheat	LNC	UAV (hyperspectral camera)	VIs Texture	RR PLSR SVR RF	R^2 = 0.84 RMSE = 0.25	[123]
Wheat	LNC LNA	ASD FieldSpec Handheld 2 RealSense depth camera D435i	VIs Canopy structural	PLS RF	LNC: R^2 = 0.78 RMSE = 0.35% LNA: R^2 = 0.79 RMSE = 1.54 g/m^2	[86]
Rice	NNI	UAV (Parrot Sequoia camera)	Spectral bands VIs	LR, SMLR RF SVM ANN	RF accuracy is the highest: R^2 = 0.61 (stem elongation stage) R^2 = 0.79 (heading stage) RMSEs = 0.09	[37]
Rice	LNC PNC LNA PNA	UAV (Cubert S185 hyperspectral camera)	Spectral bands VIs	LR, MLR PLSR ANN RF SVM	At single growth stage, LR estimation N status based on VIs has the highest accuracy; at multiple growth stages, PLSR and ML are better. RMSE = 2.1 g/m^2	[64]
Wheat	N content	HyMap sensor	Spectral bands	PROSAIL-PRO GP Heteroscedastic GP	The optimal N retrieval spectral bands are in the SWIR.	[31]
Wheat	LCC	Landsat8 ASD FieldSpec Pro	VIs	LR PROSPECT SAIL	Use hyperspectral leaf reflectance data to simulate Landsat-8 bands LR: R^2 = 0.59 PROSPECT: R^2 = 0.64	[75]
Wheat	LCC	Sentinel-2 RapidEye EnMAP	Spectral bands	PLSR	Sentinel-2: R^2 = 0.755 RapidEye: R^2 = 0.689 EnMAP: R^2 = 0.735	[74]
Wheat	LNC	ASD FieldSpec HandHeld	VIs	Statistical analysis	AIVI could overcomes the impact of VZAs: R^2 = 0.84 at −20° R^2 = 0.83 at −10° to −40°	[53]

Table 2. *Cont.*

Crop	N Status	Data Platforms	Indices	Retrieval Method	Results	References
Wheat	LNC	ASD FieldSpec	VIs Spectral bands	VIs BPNN XGBoost PLSR	$R^2 \geq 0.83$ at 0° to −30° VZAs range The accuracy of PLSR is better than VIs (16–17%), BPNN (15–16%) and XGBoost (29–58%) at VZAs ±60°	[166]
Rice	LNC_{Li}	ASD FieldSpec4	VIs	Vertical distribution model	LNC_{L1}: R^2 = 0.768 LNC_{L2}: R^2 = 0.700 LNC_{L3}: R^2 = 0.623 LNC_{L4}: R^2 = 0.549	[44]
Wheat	NNI	ASD FieldSpec Micro-Hyperspec and NIR-100 imager SC655 thermal camera	VIs Thermal indices	Statistical analysis	The combination of CCCI and DWI can overcome the influence of water to retrieve NNI, and the RMSE is reduced to 0.109.	[59]

Table 2 covers case studies from different regions.

In addition to physiological characteristics of vegetation, differences in soil background and canopy structure can cause difficulties in extracting whole leaf pixels, and noise from atmospheric transport processes also affects spectral accuracy. Existing studies mainly consider the effects of soil background and fractional vegetation cover (FVC). Before and after removing the background pixels, the accuracy of remote sensing inversion of crop biochemical parameters was significantly improved; for example, R^2 in LAI inversion could improve 0.27 [181], in N status inversion could improve 0.11 [82], and in Chl status inversion could improve 0.10 [182]. However, the applicable method of background elimination is also extremely important, as it requires high performance to adapt to the complex and changing field environment [182]. FVC correlates with background information and combining this information with spectra can also improve N estimates in different environmental contexts [183,184]. In addition, most imaging systems use top or side views to collect data, and the anisotropy of spectral information leads to different responses to crop N, and a suitable angle of spectral acquisition is important for accurate N monitoring. The blue band has atmospheric function, when the N content estimation model combined with blue band and other N-sensitive bands can improve the adaptability of the angle of data acquisition [53]. Under multiple conditions such as data acquisition, environmental stress and crop physiological stress, the spectral information is mixed with numerous non-target factors, which need to be decomposed to determine the precise response of crop N to the spectrum. Therefore, various influencing factors should be considered when estimating crop N by remote sensing to achieve high precision diagnosis.

(3) Improving the generalizability of models is key to crop N monitoring and assessment. To summarize the currently used models for inversion of N status and their effectiveness, a statistical model is currently the most commonly applied method in research experiments. When using statistical models, it is first necessary to determine the crop N indicator, the determination of which may result in experimental bias due to equipment or operational practices; subsequently, in the phase of selecting characteristic bands with high correlation to the crop N indicator, there is the possibility of wrong band selection. In essence, the reliability of statistical models to assess crop N status depends on the dataset used to train the algorithm and the model. When applied to separate datasets under different conditions, the models are less generalizable. To achieve regional scalability and explore the influence of environmental differences on modeling, datasets can be constructed by combining spectral information and ecological factors so that they contain a large amount of variability data to improve model generalizability. However, improving the predictive accuracy of the model by adjusting the input parameters still has limits. Considering the principles, there is a trade-off between model interpretation and model performance. The predictive principles of traditional statistical models are intuitive and easy to understand,

but at the expense of model performance; some machine learning models produce better predictive accuracy, while they are considered black box models because explaining how these models make decisions is a very difficult task (partial model prediction accuracy show in Table 2).

Physical models are highly advantageous in achieving model generalization, as they simulate the interaction between physical–chemical parameters and light from the physiological mechanisms of crops, thus providing explanations for the complex relationships between spectra and physical–chemical parameters at different fertility periods and under different growing conditions. However, the tedious and time-consuming inversion process limits its application. Existing studies usually analyze crop status at a small number of growth stages, so the statistical model has limited transferability across crops with different phenological status. The physical model overcomes this limitation and allows a wider range of crop canopy properties to be simulated. A hybrid model combining the mechanisms of statistical and physical models is not only efficient and flexible, but also explanatory for parameter inversion. In a hybrid model, the physical model is used to generate simulated spectra, which describes intra-canopy radiative transfer and interactions according to physics laws, thus providing information on spectral reflectance in relation to crop physicochemical variables [28]. Using simulated spectral data as input to train statistical models can provide physical constraints and explanations, and give a wider range of suitability [185]. Hybrid models have been applied successfully to estimate crop physical–chemical parameters (LAI, LCC, FVC, etc.) [185–187], but have rarely been used to invert N status. In recent years, physical models have moved from the previous indirect inversion of N through the physiological relationship between Chl and N to explore direct modeling of crop N status from spectral information, with more stable models and high response efficiency. Berger et al. [31] and Verrelst et al. [158] combined GP and PROSAIL-PRO models for inversion of crop N content, and confirmed the efficiency of hybrid models for direct N estimation. Therefore, how to achieve the complementary advantages between statistical and physical models, then construct a crop N estimation model with both mechanics and accuracy, will be the focus of future research.

6. Conclusions

Remote sensing technology is developing at a rapid pace and non-destructive monitoring and assessment of crop N status is gaining importance. This paper analyses the physiological mechanisms and spectral response characteristics of remote sensing monitoring for canopy N. Taking the remote sensing monitoring platform, the correlation between remotely sensed data and N status, and the remote sensing retrieval methods as the entry point, this paper provides an in-depth summary of the research techniques in the field of remote sensing monitoring for canopy N. The factors affecting the accuracy of remote sensing monitoring are also discussed. To date, the research at field scale has been well validated. The development of sensors and spectral carrying platforms facilitates high-precision remote sensing monitoring of crop N at farm scale. Due to the amount of information that can be extracted from remote sensing data, the efficiency of model use has become a key research concern. The efficiency and flexibility of machine learning models and the explanatory nature of physical models have their own advantages. The hybrid of the two models is beginning to show results in improving model stability. In addition, the effective use of multi-source data, and the removal of confounding factors in crop N monitoring need to be further explored. In-depth understanding of the limitations of current technology will be necessary to enhance the understanding of the link between canopy optical properties and crop N status, and to identify more appropriate N retrieval methods. In the context of the current rapid development of smart agriculture, the combination of sensors, remote sensing platforms and the Internet of Things results in the initial formation of a crop growth monitoring IoT platform. It provides the development direction for real-time monitoring and early forecasting of crop N, making it more widely application in the fields of growth monitoring, yield prediction and precision fertilization.

Author Contributions: Conceptualization, J.Z. and X.Y.; writing—original draft preparation, J.Z. and X.Y.; writing—review and editing, X.S., G.Y., X.D. and X.M. All authors have read and agreed to the published version of the manuscript.

Funding: This research was funded by Science and Technology Department of Guangdong Province (2019B020216001) and National Key Research and Development of China (2019YFE0125300).

Data Availability Statement: Not applicable.

Conflicts of Interest: The authors declare no conflict of interest.

References

1. Miao, Y.; Stewart, B.A.; Zhang, F. Long-term experiments for sustainable nutrient management in China. A review. *Agron. Sustain. Dev.* **2011**, *31*, 397–414. [CrossRef]
2. Liang, G.; Sun, P.; Waring, B.G. Nitrogen agronomic efficiency under nitrogen fertilization does not change over time in the long term: Evidence from 477 global studies. *Soil Tillage Res.* **2022**, *223*, 105468. [CrossRef]
3. Diacono, M.; Rubino, P.; Montemurro, F. Precision nitrogen management of wheat. A review. *Agron. Sustain. Dev.* **2013**, *33*, 219–241. [CrossRef]
4. Lu, J.J.; Wang, H.Y.; Miao, Y.X.; Zhao, L.Q.; Zhao, G.M.; Cao, Q.; Kusnierek, K. Developing an active canopy sensor-based integrated precision rice management system for improving grain yield and quality, nitrogen use efficiency, and lodging resistance. *Remote Sens.* **2022**, *14*, 2440. [CrossRef]
5. Chang, J.F.; Havlik, P.; Leclere, D.; de Vries, W.; Valin, H.; Deppermann, A.; Hasegawa, T.; Obersteiner, M. Reconciling regional nitrogen boundaries with global food security. *Nat. Food* **2021**, *2*, 700–711. [CrossRef]
6. Ren, K.; Xu, M.; Li, R.; Zheng, L.; Liu, S.; Reis, S.; Wang, H.; Lu, C.; Zhang, W.; Gao, H.; et al. Optimizing nitrogen fertilizer use for more grain and less pollution. *J. Clean. Prod.* **2022**, *360*, 132180. [CrossRef]
7. Yang, G.J.; Zhao, C.J.; Li, Z.H. *Quantitative Remote Sensing of Crop Nitrogen Nutrition and Its Application*; Science Press: Beijing, China, 2019.
8. Andrews, M.; Raven, J.A.; Lea, P.J. Do plants need nitrate? The mechanisms by which nitrogen form affects plants. *Ann. Appl. Biol.* **2013**, *163*, 174–199. [CrossRef]
9. Li, D.; Tian, M.; Cai, J.; Jiang, D.; Cao, W.; Dai, T. Effects of low nitrogen supply on relationships between photosynthesis and nitrogen status at different leaf position in wheat seedlings. *Plant Growth Regul.* **2013**, *70*, 257–263. [CrossRef]
10. Wang, L.; Xue, C.; Pan, X.; Chen, F.; Liu, Y. Application of controlled-release urea enhances grain yield and nitrogen use efficiency in irrigated rice in the Yangtze River Basin, China. *Front. Plant Sci.* **2018**, *9*, 999. [CrossRef]
11. Fu, Y.; Yang, G.; Li, Z.; Song, X.; Li, Z.; Xu, X.; Wang, P.; Zhao, C. Winter wheat nitrogen status estimation using UAV-based RGB imagery and gaussian processes regression. *Remote Sens.* **2020**, *12*, 3778. [CrossRef]
12. Moharana, S.; Dutta, S. Spatial variability of chlorophyll and nitrogen content of rice from hyperspectral imagery. *ISPRS J. Photogramm. Remote Sens.* **2016**, *122*, 17–29. [CrossRef]
13. Thorp, K.R.; Wang, G.; Bronson, K.F.; Badaruddin, M.; Mon, J. Hyperspectral data mining to identify relevant canopy spectral features for estimating durum wheat growth, nitrogen status, and grain yield. *Comput. Electron. Agric.* **2017**, *136*, 1–12. [CrossRef]
14. Fu, Y.; Yang, G.; Pu, R.; Li, Z.; Li, H.; Xu, X.; Song, X.; Yang, X.; Zhao, C. An overview of crop nitrogen status assessment using hyperspectral remote sensing: Current status and perspectives. *Eur. J. Agron.* **2021**, *124*, 126241. [CrossRef]
15. Sun, J.; Shi, S.; Wang, L.; Li, H.; Wang, S.; Gong, W.; Tagesson, T. Optimizing LUT-based inversion of leaf chlorophyll from hyperspectral lidar data: Role of cost functions and regulation strategies. *Int. J. Appl. Earth Obs. Geoinf.* **2021**, *105*, 102602. [CrossRef]
16. Vigneau, N.; Ecarnot, M.; Rabatel, G.; Roumet, P. Potential of field hyperspectral imaging as a non destructive method to assess leaf nitrogen content in Wheat. *Field Crops Res.* **2011**, *122*, 25–31. [CrossRef]
17. Shao, Y.; Zhao, C.; Bao, Y.; He, Y. Quantification of nitrogen status in rice by least squares support vector machines and reflectance spectroscopy. *Food Bioprocess Technol.* **2012**, *5*, 100–107. [CrossRef]
18. Li, S.; Ji, W.; Chen, S.; Peng, J.; Zhou, Y.; Shi, Z. Potential of VIS-NIR-SWIR spectroscopy from the Chinese soil spectral library for assessment of nitrogen fertilization rates in the paddy-rice region, China. *Remote Sens.* **2015**, *7*, 7029–7043. [CrossRef]
19. Maes, W.H.; Steppe, K. Perspectives for remote sensing with unmanned aerial vehicles in precision agriculture. *Trends Plant Sci.* **2019**, *24*, 152–164. [CrossRef]
20. Inoue, Y.; Sakaiya, E.; Zhu, Y.; Takahashi, W. Diagnostic mapping of canopy nitrogen content in rice based on hyperspectral measurements. *Remote Sens. Environ.* **2012**, *126*, 210–221. [CrossRef]
21. Kattenborn, T.; Schiefer, F.; Zarco-Tejada, P.; Schmidtlein, S. Advantages of retrieving pigment content [µg/cm2] versus concentration [%] from canopy reflectance. *Remote Sens. Environ.* **2019**, *230*, 111195. [CrossRef]
22. Cai, C.; Li, G.; Di, L.; Ding, Y.; Fu, L.; Guo, X.; Struik, P.C.; Pan, G.; Li, H.; Chen, W.; et al. The acclimation of leaf photosynthesis of wheat and rice to seasonal temperature changes in T-FACE environments. *Glob. Chang. Biol.* **2020**, *26*, 539–556. [CrossRef] [PubMed]

23. Boogaard, H.; Van Diepen, C.; Rotter, R.; Cabrera, J.; Van Laar, H. *WOFOST 7.1: User's Guide for the WOFOST 7.1 Crop Growth Simulation Model and WOFOST Control Center 1.5*; Wageningen University & Research: Wageningen, The Netherlands, 1998.
24. Li, D.; Chen, J.M.; Yan, Y.; Zheng, H.; Yao, X.; Zhu, Y.; Cao, W.; Cheng, T. Estimating leaf nitrogen content by coupling a nitrogen allocation model with canopy reflectance. *Remote Sens. Environ.* **2022**, *283*, 113314. [CrossRef]
25. Ohyama, T. Nitrogen as a major essential element of plants. *Nitrogen Assim. Plants* **2010**, *37*, 2–17.
26. Wang, Y.-P.; Chang, Y.-C.; Shen, Y. Estimation of nitrogen status of paddy rice at vegetative phase using unmanned aerial vehicle based multispectral imagery. *Precis. Agric.* **2022**, *23*, 1–17. [CrossRef]
27. Li, D.; Wang, X.; Zheng, H.; Zhou, K.; Yao, X.; Tian, Y.; Zhu, Y.; Cao, W.; Cheng, T. Estimation of area- and mass-based leaf nitrogen contents of wheat and rice crops from water-removed spectra using continuous wavelet analysis. *Plant Methods* **2018**, *14*, 76. [CrossRef]
28. Berger, K.; Verrelst, J.; Feret, J.-B.; Wang, Z.; Wocher, M.; Strathmann, M.; Danner, M.; Mauser, W.; Hank, T. Crop nitrogen monitoring: Recent progress and principal developments in the context of imaging spectroscopy missions. *Remote Sens. Environ.* **2020**, *242*, 111758. [CrossRef]
29. Botha, E.J.; Leblon, B.; Zebarth, B.J.; Watmough, J. Non-destructive estimation of wheat leaf chlorophyll content from hyperspectral measurements through analytical model inversion. *Int. J. Remote Sens.* **2010**, *31*, 1679–1697. [CrossRef]
30. Feret, J.-B.; Berger, K.; de Boissieu, F.; Malenovsky, Z. PROSPECT-PRO for estimating content of nitrogen-containing leaf proteins and other carbon-based constituents. *Remote Sens. Environ.* **2021**, *252*, 112173. [CrossRef]
31. Berger, K.; Verrelst, J.; Feret, J.-B.; Hank, T.; Wocher, M.; Mauser, W.; Camps-Valls, G. Retrieval of aboveground crop nitrogen content with a hybrid machine learning method. *Int. J. Appl. Earth Obs. Geoinf.* **2020**, *92*, 102174. [CrossRef]
32. Zhu, Y.; Yao, X.; Tian, Y.; Liu, X.; Cao, W. Analysis of common canopy vegetation indices for indicating leaf nitrogen accumulations in wheat and rice. *Int. J. Appl. Earth Obs. Geoinf.* **2008**, *10*, 1–10. [CrossRef]
33. Fitzgerald, G.J.; Rodriguez, D.; Christensen, L.K.; Belford, R.; Sadras, V.O.; Clarke, T.R. Spectral and thermal sensing for nitrogen and water status in rainfed and irrigated wheat environments. *Precis. Agric.* **2006**, *7*, 233–248. [CrossRef]
34. Zhu, Y.; Tian, Y.; Yao, X.; Liu, X.; Cao, W. Analysis of common canopy reflectance spectra for indicating leaf nitrogen concentrations in wheat and rice. *Plant Prod. Sci.* **2007**, *10*, 400–411. [CrossRef]
35. Hua, Q.; Yu, Y.; Dong, S.; Li, S.; Shen, H.; Han, Y.; Zhang, J.; Xiao, J.; Liu, S.; Dong, Q.; et al. Leaf spectral responses of Poa crymophila to nitrogen deposition and climate change on Qinghai-Tibetan Plateau. *Agric. Ecosyst. Environ.* **2019**, *284*, 106598. [CrossRef]
36. Tang, Y.L.; Wang, R.C.; Huang, J.F. Relations between red edge characteristics and agronomic parameters of crops. *Pedosphere* **2004**, *14*, 467–474.
37. Zha, H.; Miao, Y.; Wang, T.; Li, Y.; Zhang, J.; Sun, W.; Feng, Z.; Kusnierek, K. Improving unmanned aerial vehicle remote sensing-based rice nitrogen nutrition index prediction with machine learning. *Remote Sens.* **2020**, *12*, 215. [CrossRef]
38. Wang, W.; Yao, X.; Tian, Y.-C.; Liu, X.-J.; Ni, J.; Cao, W.-X.; Zhu, Y. Common spectral bands and optimum vegetation indices for monitoring leaf nitrogen accumulation in rice and wheat. *J. Integr. Agric.* **2012**, *11*, 2001–2012. [CrossRef]
39. Nguyen, H.T.; Lee, B.W. Assessment of rice leaf growth and nitrogen status by hyperspectral canopy reflectance and partial least square regression. *Eur. J. Agron.* **2006**, *24*, 349–356. [CrossRef]
40. He, J.; Ma, J.; Cao, Q.; Wang, X.; Yao, X.; Cheng, T.; Zhu, Y.; Cao, W.; Tian, Y. Development of critical nitrogen dilution curves for different leaf layers within the rice canopy. *Eur. J. Agron.* **2022**, *132*, 126414. [CrossRef]
41. Li, H.; Zhao, C.; Huang, W.; Yang, G. Non-uniform vertical nitrogen distribution within plant canopy and its estimation by remote sensing: A review. *Field Crops Res.* **2013**, *142*, 75–84. [CrossRef]
42. Wang, J.H.; Wang, Z.J.; Huang, W.J.; Ma, Z.H.; Liu, L.Y.; Zhao, C.J. The vertical dist ribution characteristic and spectral response of canopy nitrogen in different layer of winter wheat. *Natl. Remote Sens. Bull.* **2004**, *8*, 309–316.
43. Duan, D.-D.; Zhao, C.-J.; Li, Z.-H.; Yang, G.-J.; Zhao, Y.; Qiao, X.-J.; Zhang, Y.-H.; Zhang, L.-X.; Yang, W.-D. Estimating total leaf nitrogen concentration in winter wheat by canopy hyperspectral data and nitrogen vertical distribution. *J. Integr. Agric.* **2019**, *18*, 1562–1570. [CrossRef]
44. He, J.; Zhang, X.; Guo, W.; Pan, Y.; Yao, X.; Cheng, T.; Zhu, Y.; Cao, W.; Tian, Y. Estimation of vertical leaf nitrogen distribution within a rice canopy based on hyperspectral data. *Front. Plant Sci.* **2020**, *10*, 1802. [CrossRef] [PubMed]
45. Camino, C.; Gonzalez-Dugo, V.; Hernandez, P.; Sillero, J.C.; Zarco-Tejada, P.J. Improved nitrogen retrievals with airborne-derived fluorescence and plant traits quantified from VNIR-SWIR hyperspectral imagery in the context of precision agriculture. *Int. J. Appl. Earth Obs. Geoinf.* **2018**, *70*, 105–117. [CrossRef]
46. Aranguren, M.; Castellon, A.; Aizpurua, A. Crop sensor based non-destructive estimation of nitrogen nutritional status, yield, and grain protein content in wheat. *Agriculture* **2020**, *10*, 148. [CrossRef]
47. Staenz, K.; Secker, J.; Gao, B.C.; Davis, C.; Nadeau, C. Radiative transfer codes applied to hyperspectral data for the retrieval of surface reflectance. *ISPRS J. Photogramm. Remote Sens.* **2002**, *57*, 194–203. [CrossRef]
48. Peron-Danaher, R.; Russell, B.; Cotrozzi, L.; Mohammadi, M.; Couture, J. Incorporating multi-scale, spectrally detected nitrogen concentrations into assessing nitrogen use efficiency for winter wheat breeding populations. *Remote Sens.* **2021**, *13*, 3991. [CrossRef]

49. Jiang, X.; Zhen, J.; Miao, J.; Zhao, D.; Shen, Z.; Jiang, J.; Gao, C.; Wu, G.; Wang, J. Newly-developed three-band hyperspectral vegetation index for estimating leaf relative chlorophyll content of mangrove under different severities of pest and disease. *Ecol. Indic.* **2022**, *140*, 108978. [CrossRef]
50. Xiong, Y.; Liu, B.; Yue, Y. Inversion of nitrogen content of plant leaves based on ASD and FISS. *Ecol. Environ. Sci.* **2013**, *22*, 582–587.
51. Jiang, J.; Zhang, Z.; Cao, Q.; Liang, Y.; Krienke, B.; Tian, Y.; Zhu, Y.; Cao, W.; Liu, X. Use of an active canopy sensor mounted on an unmanned aerial vehicle to monitor the growth and nitrogen status of winter wheat. *Remote Sens.* **2020**, *12*, 3684. [CrossRef]
52. Wang, J.; Xu, B.; Wang, C.; Yang, G.; Yang, Z.; Mei, X.; Yang, X. Design and application of data acquisition and analysis system for CropSense. *Smart Agric.* **2019**, *1*, 91–104.
53. He, L.; Song, X.; Feng, W.; Guo, B.B.; Zhang, Y.S.; Wang, Y.H.; Wang, C.Y.; Guo, T.C. Improved remote sensing of leaf nitrogen concentration in winter wheat using multi-angular hyperspectral data. *Remote Sens. Environ.* **2016**, *174*, 122–133. [CrossRef]
54. Wu, B.; Huang, W.; Ye, H.; Luo, P.; Ren, Y.; Kong, W. Using multi-angular hyperspectral data to estimate the vertical distribution of leaf chlorophyll content in wheat. *Remote Sens.* **2021**, *13*, 1501. [CrossRef]
55. Liao, Q.; Zhang, D.; Wang, J.; Yang, G.; Yang, H.; Craig, C.; Wong, Z.; Wang, D. Assessment of chlorophyli content using a new vegetation index based on multi-angular hyperspectral image data. *Spectrosc. Spectr. Anal.* **2014**, *34*, 1599–1604.
56. Sun, J.; Shi, S.; Gong, W.; Yang, J.; Du, L.; Song, S.; Chen, B.; Zhang, Z. Evaluation of hyperspectral LiDAR for monitoring rice leaf nitrogen by comparison with multispectral LiDAR and passive spectrometer. *Sci. Rep.* **2017**, *7*, 40362. [CrossRef]
57. Huang, S.; Miao, Y.; Yuan, F.; Cao, Q.; Ye, H.; Lenz-Wiedemann, V.I.S.; Bareth, G. In-season diagnosis of rice nitrogen status using proximal fluorescence canopy sensor at different growth stages. *Remote Sens.* **2019**, *11*, 1847. [CrossRef]
58. Du, L.; Gong, W.; Yang, J. Application of spectral indices and reflectance spectrum on leaf nitrogen content analysis derived from hyperspectral LiDAR data. *Opt. Laser Technol.* **2018**, *107*, 372–379. [CrossRef]
59. Pancorbo, J.L.; Camino, C.; Alonso-Ayuso, M.; Raya-Sereno, M.D.; Gonzalez-Fernandez, I.; Gabriel, J.L.; Zarco-Tejada, P.J.; Quemada, M. Simultaneous assessment of nitrogen and water status in winter wheat using hyperspectral and thermal sensors. *Eur. J. Agron.* **2021**, *127*, 126287. [CrossRef]
60. Zhang, J.; Qiu, X.; Wu, Y.; Zhu, Y.; Cao, Q.; Liu, X.; Cao, W. Combining texture, color, and vegetation indices from fixed-wing UAS imagery to estimate wheat growth parameters using multivariate regression methods. *Comput. Electron. Agric.* **2021**, *185*, 106138. [CrossRef]
61. Oppelt, N.; Mauser, W. Hyperspectral monitoring of physiological parameters of wheat during a vegetation period using AVIS data. *Int. J. Remote Sens.* **2004**, *25*, 145–159. [CrossRef]
62. Lu, B.; Dao, P.D.; Liu, J.; He, Y.; Shang, J. Recent advances of hyperspectral imaging technology and applications in agriculture. *Remote Sens.* **2020**, *12*, 2659. [CrossRef]
63. Zhu, H.; Liu, H.; Xu, Y.; Yang, G. UAV-based hyperspectral analysis and spectral indices constructing for quantitatively monitoring leaf nitrogen content of winter wheat. *Appl. Opt.* **2018**, *57*, 7722–7732. [CrossRef] [PubMed]
64. Wang, L.; Chen, S.; Li, D.; Wang, C.; Jiang, H.; Zheng, Q.; Peng, Z. Estimation of paddy rice nitrogen content and accumulation both at leaf and plant levels from UAV hyperspectral imagery. *Remote Sens.* **2021**, *13*, 2956. [CrossRef]
65. Yi, X.; Lan, A.; Wen, X.; Zhang, Y.; Li, Y. Monitoring of heavy metals in farmland soils based on ASD and GaiaSky-mini. *Chin. J. Ecol.* **2018**, *37*, 1781–1788.
66. Wan, L.; Cen, H.; Zhu, J.; Zhang, J.; Du, X.; He, Y. Using fusion of texture features and vegetation indices from water concentration in rice crop to UAV remote sensing monitor. *Smart Agric.* **2020**, *2*, 58–67.
67. Zhu, J.; Cen, H.; He, L.; He, Y. Development and performance evaluation of a multi-rotor unmanned aircraft system for agricultural monitoring. *Smart Agric.* **2019**, *1*, 43–52.
68. Delloye, C.; Weiss, M.; Defourny, P. Retrieval of the canopy chlorophyll content from Sentinel-2 spectral bands to estimate nitrogen uptake in intensive winter wheat cropping systems. *Remote Sens. Environ.* **2018**, *216*, 245–261. [CrossRef]
69. Zhao, H.; Song, X.; Yang, G.; Li, Z.; Zhang, D.; Feng, H. Monitoring of nitrogen and grain protein content in winter wheat based on Sentinel-2A data. *Remote Sens.* **2019**, *11*, 1724. [CrossRef]
70. Houborg, R.; Cescatti, A.; Migliavacca, M.; Kustas, W.P. Satellite retrievals of leaf chlorophyll and photosynthetic capacity for improved modeling of GPP. *Agric. For. Meteorol.* **2013**, *177*, 10–23. [CrossRef]
71. Hunt, E.R., Jr.; Doraiswamy, P.C.; McMurtrey, J.E.; Daughtry, C.S.T.; Perry, E.M.; Akhmedov, B. A visible band index for remote sensing leaf chlorophyll content at the canopy scale. *Int. J. Appl. Earth Obs. Geoinf.* **2013**, *21*, 103–112. [CrossRef]
72. Huang, S.; Miao, Y.; Yuan, F.; Gnyp, M.L.; Yao, Y.; Cao, Q.; Wang, H.; Lenz-Wiedemann, V.I.S.; Bareth, G. Potential of RapidEye and WorldView-2 satellite data for improving rice nitrogen status monitoring at different growth stages. *Remote Sens.* **2017**, *9*, 227. [CrossRef]
73. Magney, T.S.; Eitel, J.U.H.; Vierling, L.A. Mapping wheat nitrogen uptake from RapidEye vegetation indices. *Precis. Agric.* **2017**, *18*, 429–451. [CrossRef]
74. Cui, B.; Zhao, Q.-J.; Huang, W.-J.; Song, X.-Y.; Ye, H.-C.; Zhou, X.-F. Leaf chlorophyll content retrieval of wheat by simulated RapidEye, Sentinel-2 and EnMAP data. *J. Integr. Agric.* **2019**, *18*, 1230–1245. [CrossRef]
75. Croft, H.; Arabian, J.; Chen, J.M.; Shang, J.; Liu, J. Mapping within-field leaf chlorophyll content in agricultural crops for nitrogen management using Landsat-8 imagery. *Precis. Agric.* **2020**, *21*, 856–880. [CrossRef]
76. Yao, X.; Liu, X.J.; Tian, Y.C.; Cao, W.X.; Zhu, Y.; Zhang, Y. Quantitative relationships between satellite channels-based spectral parameters and wheat canopy leaf nitrogen status. *Chin. J. Appl. Ecol.* **2013**, *24*, 431–437.

77. Tan, C.; Zhou, J.; Luo, M.; Du, Y.; Yang, X.; Ma, C. Using combined vegetation indices to monitor leaf chlorophyll content in winter wheat based on Hj-1a/1b images. *Int. J. Agric. Biol.* **2017**, *19*, 1576–1584.
78. Jiang, X.; Fang, S.; Huang, X.; Liu, Y.; Guo, L. Rice mapping and growth monitoring based on time series GF-6 images and red-edge bands. *Remote Sens.* **2021**, *13*, 579. [CrossRef]
79. Kang, Y.; Meng, Q.; Liu, M.; Zou, Y.; Wang, X. Crop classification based on red edge features analysis of GF-6 WFV data. *Sensors* **2021**, *21*, 4328. [CrossRef]
80. Xia, T.; He, Z.; Cai, Z.; Wang, C.; Wang, W.; Wang, J.; Hu, Q.; Song, Q. Exploring the potential of Chinese GF-6 images for crop mapping in regions with complex agricultural landscapes. *Int. J. Appl. Earth Obs. Geoinf.* **2022**, *107*, 102702. [CrossRef]
81. Wang, C.; Zhang, X.; Shi, T.; Zhang, C.; Li, M. Classification of medicinal plants astragalus mongholicus bunge and sophora flavescens aiton using GaoFen-6 and multitemporal Sentinel-2 data. *IEEE Geosci. Remote Sens. Lett.* **2022**, *19*, 2502805. [CrossRef]
82. Chen, P.; Liang, F. Cotton nitrogen nutrition diagnosis based on spectrum and texture feature of images from low altitude unmanned aerial vehicle. *Sci. Agric. Sin.* **2019**, *52*, 2220–2229, (In Chinese with English Abstract).
83. Yu, Z.; Wang, J.I.; Chen, L.I.; Fu, Y.U.; Zhu, H.O.; Feng, H.A.; Xu, X.I.; Li, Z.H. An entirely new approach based on remote sensing data to calculate the nitrogen nutrition index of winter wheat. *J. Integr. Agric.* **2021**, *20*, 2535–2551.
84. Justes, E.; Mary, B.; Meynard, J.M.; Machet, J.M.; Thelier-Huche, L. Determination of a critical nitrogen dilution curve for winter wheat crops. *Ann. Bot.* **1994**, *74*, 397–407. [CrossRef]
85. Zheng, H.; Ma, J.; Zhou, M.; Li, D.; Yao, X.; Cao, W.; Zhu, Y.; Cheng, T. Enhancing the nitrogen signals of rice canopies across critical growth stages through the integration of textural and spectral information from Unmanned Aerial Vehicle (UAV) multispectral imagery. *Remote Sens.* **2020**, *12*, 957. [CrossRef]
86. Li, H.; Li, D.; Xu, K.; Cao, W.; Jiang, X.; Ni, J. Monitoring of nitrogen indices in wheat leaves based on the integration of spectral and canopy structure information. *Agronomy* **2022**, *12*, 833. [CrossRef]
87. Zhou, K.; Cheng, T.; Zhu, Y.; Cao, W.; Ustin, S.L.; Zheng, H.; Yao, X.; Tian, Y. Assessing the impact of spatial resolution on the estimation of leaf nitrogen concentration over the full season of paddy rice using near-surface imaging spectroscopy data. *Front. Plant Sci.* **2018**, *9*, 964. [CrossRef]
88. Zheng, H.; Cheng, T.; Li, D.; Zhou, X.; Yao, X.; Tian, Y.; Cao, W.; Zhu, Y. Evaluation of RGB, color-infrared and multispectral images acquired from unmanned aerial systems for the estimation of nitrogen accumulation in rice. *Remote Sens.* **2018**, *10*, 824. [CrossRef]
89. Hansen, P.M.; Schjoerring, J.K. Reflectance measurement of canopy biomass and nitrogen status in wheat crops using normalized difference vegetation indices and partial least squares regression. *Remote Sens. Environ.* **2003**, *86*, 542–553. [CrossRef]
90. Dunn, B.W.; Dehaan, R.; Schmidtke, L.M.; Dunn, T.S.; Meder, R. Using field-derived hyperspectral reflectance measurement to identify the essential wavelengths for predicting nitrogen uptake of rice at panicle initiation. *J. Near Infrared Spectrosc.* **2016**, *24*, 473–483. [CrossRef]
91. Feng, M.-C.; Zhao, J.-J.; Yang, W.-D.; Wang, C.; Zhang, M.-J.; Xiao, L.-J.; Ding, G.-W. Evaluating winter wheat (*Triticum aestivum* L.) nitrogen status using canopy spectrum reflectance and multiple statistical analysis. *Spectrosc. Lett.* **2016**, *49*, 507–513. [CrossRef]
92. Tan, C.; Du, Y.; Zhou, J.; Wang, D.; Luo, M.; Zhang, Y.; Guo, W. Analysis of different hyperspectral variables for diagnosing leaf nitrogen accumulation in wheat. *Front. Plant Sci.* **2018**, *9*, 674. [CrossRef]
93. Wang, J.-J.; Song, X.-Y.; Mei, X.; Yang, G.-J.; Li, Z.-H.; Li, H.-L.; Meng, Y. Sensitive bands selection and nitrogen content monitoring of rice based on gaussian regression analysis. *Spectrosc. Spectr. Anal.* **2021**, *41*, 1722–1729.
94. Yu, F.; Feng, S.; Du, W.; Wang, D.; Guo, Z.; Xing, S.; Jin, Z.; Cao, Y.; Xu, T. A study of nitrogen deficiency inversion in rice leaves based on the hyperspectral reflectance differential. *Front. Plant Sci.* **2020**, *11*, 573272. [CrossRef] [PubMed]
95. Liu, T.; Xu, T.; Yu, F.; Yuan, Q.; Guo, Z.; Xu, B. A method combining ELM and PLSR (ELM-P) for estimating chlorophyll content in rice with feature bands extracted by an improved ant colony optimization algorithm. *Comput. Electron. Agric.* **2021**, *186*, 106177. [CrossRef]
96. Yang, B.; Chen, J.; Chen, L.; Cao, W.; Yao, X.; Zhu, Y. Estimation model of wheat canopy nitrogen content based on sensitive bands. *Trans. Chin. Soc. Agric. Eng.* **2015**, *31*, 176–182.
97. Cao, Y.L.; Xiao, W.; Liu, Y.D.; Jiang, K.L.; Guo, B.Y.; Yu, F.H. Dimension reduction of hyperspectral data and analysis of rice nitrogen content. *J. Shenyang Agric. Univ.* **2021**, *52*, 109–115.
98. Liu, H.; Zhu, H.; Wang, P. Quantitative modelling for leaf nitrogen content of winter wheat using UAV-based hyperspectral data. *Int. J. Remote Sens.* **2017**, *38*, 2117–2134. [CrossRef]
99. Lu, J.; Li, W.; Yu, M.; Zhang, X.; Ma, Y.; Su, X.; Yao, X.; Cheng, T.; Zhu, Y.; Cao, W.; et al. Estimation of rice plant potassium accumulation based on non-negative matrix factorization using hyperspectral reflectance. *Precis. Agric.* **2021**, *22*, 51–74. [CrossRef]
100. Xu, X.G.; Zhao, C.J.; Wang, J.H.; Li, C.J.; Yang, X.D. Associating new spectral features from visible and near infrared regions with optimal combination principle to monitor leaf nitrogen concentration in barley. *J. Infrared Millim. Waves* **2013**, *32*, 351–358+365. [CrossRef]
101. An, G.; Xing, M.; He, B.; Liao, C.; Huang, X.; Shang, J.; Kang, H. Using machine learning for estimating rice chlorophyll content from in situ hyperspectral data. *Remote Sens.* **2020**, *12*, 3104. [CrossRef]
102. Boochs, F.; Kupfer, G.; Dockter, K.; Kühbauch, W. Shape of the red edge as vitality indicator for plants. *Remote Sens.* **1990**, *11*, 1741–1753. [CrossRef]

103. Horler, D.N.H.; Barber, J.; Barringer, A.R. Effects of heavy metals on the absorbance and reflectance spectra of plants. *Int. J. Remote Sens.* **1980**, *1*, 121–136. [CrossRef]
104. Feng, W.; Yao, X.; Zhu, Y.; Tian, Y.C.; Cao, W. Monitoring leaf nitrogen status with hyperspectral reflectance in wheat. *Eur. J. Agron.* **2008**, *28*, 394–404. [CrossRef]
105. Tian, Y.; Yao, X.; Yang, J.; Cao, W.; Zhu, Y. Extracting red edge position parameters from ground- and space-based hyperspectral data for estimation of canopy leaf nitrogen concentration in rice. *Plant Prod. Sci.* **2011**, *14*, 270–281. [CrossRef]
106. Li, D.; Cheng, T.; Zhou, K.; Zheng, H.; Yao, X.; Tian, Y.; Zhu, Y.; Cao, W. WREP: A wavelet-based technique for extracting the red edge position from reflectance spectra for estimating leaf and canopy chlorophyll contents of cereal crops. *ISPRS J. Photogramm. Remote Sens.* **2017**, *129*, 103–117. [CrossRef]
107. Guo, B.-B.; Qi, S.-L.; Heng, Y.-R.; Duan, J.-Z.; Zhang, H.-Y.; Wu, Y.-P.; Feng, W.; Xie, Y.-X.; Zhu, Y.-J. Remotely assessing leaf N uptake in winter wheat based on canopy hyperspectral red-edge absorption. *Eur. J. Agron.* **2017**, *82*, 113–124. [CrossRef]
108. Blackburn, G.A. Wavelet decomposition of hyperspectral data: A novel approach to quantifying pigment concentrations in vegetation. *Int. J. Remote Sens.* **2007**, *28*, 2831–2855. [CrossRef]
109. Guo, J.; Zhang, J.; Xiong, S.; Zhang, Z.; Wei, Q.; Zhang, W.; Feng, W.; Ma, X. Hyperspectral assessment of leaf nitrogen accumulation for winter wheat using different regression modeling. *Precis. Agric.* **2021**, *22*, 1634–1658. [CrossRef]
110. Liang, T.; Duan, B.; Luo, X.; Ma, Y.; Yuan, Z.; Zhu, R.; Peng, Y.; Gong, Y.; Fang, S.; Wu, X. Identification of high nitrogen use efficiency phenotype in rice (*Oryza sativa* L.) through entire growth duration by unmanned aerial vehicle multispectral imagery. *Front. Plant Sci.* **2021**, *12*, 740414. [CrossRef]
111. Cui, B.; Zhao, Q.; Huang, W.; Song, X.; Ye, H.; Zhou, X. A new integrated vegetation index for the estimation of winter wheat leaf chlorophyll content. *Remote Sens.* **2019**, *11*, 974. [CrossRef]
112. Zhu, Y.; Zhou, D.; Yao, X.; Tian, Y.; Cao, W. Quantitative relationships of leaf nitrogen status to canopy spectral reflectance in rice. *Aust. J. Agric. Res.* **2007**, *58*, 1077–1085. [CrossRef]
113. Wang, W.; Yao, X.; Yao, X.; Tian, Y.; Liu, X.; Ni, J.; Cao, W.; Zhu, Y. Estimating leaf nitrogen concentration with three-band vegetation indices in rice and wheat. *Field Crops Res.* **2012**, *129*, 90–98. [CrossRef]
114. Tian, Y.C.; Yao, X.; Yang, J.; Cao, W.X.; Hannaway, D.B.; Zhu, Y. Assessing newly developed and published vegetation indices for estimating rice leaf nitrogen concentration with ground- and space-based hyperspectral reflectance. *Field Crops Res.* **2011**, *120*, 299–310. [CrossRef]
115. Yao, Y.; Miao, Y.; Cao, Q.; Wang, H.; Gnyp, M.L.; Bareth, G.; Khosla, R.; Yang, W.; Liu, F.; Liu, C. In-season estimation of rice nitrogen status with an active crop canopy sensor. *IEEE J. Sel. Top. Appl. Earth Obs. Remote Sens.* **2014**, *7*, 4403–4413. [CrossRef]
116. Wang, W.; Wu, Y.; Zhang, Q.; Zheng, H.; Yao, X.; Zhu, Y.; Cao, W.; Cheng, T. AAVI: A novel approach to estimating leaf nitrogen concentration in rice from unmanned aerial vehicle multispectral imagery at early and middle growth stages. *IEEE J. Sel. Top. Appl. Earth Obs. Remote Sens.* **2021**, *14*, 6716–6728. [CrossRef]
117. Patel, M.K.; Ryu, D.; Western, A.W.; Suter, H.; Young, I.M. Which multispectral indices robustly measure canopy nitrogen across seasons: Lessons from an irrigated pasture crop. *Comput. Electron. Agric.* **2021**, *182*, 106000. [CrossRef]
118. Li, F.; Mistele, B.; Hu, Y.; Yue, X.; Yue, S.; Miao, Y.; Chen, X.; Cui, Z.; Meng, Q.; Schmidhalter, U. Remotely estimating aerial N status of phenologically differing winter wheat cultivars grown in contrasting climatic and geographic zones in China and Germany. *Field Crops Res.* **2012**, *138*, 21–32. [CrossRef]
119. Palka, M.; Manschadi, A.M.; Koppensteiner, L.; Neubauer, T.; Fitzgerald, G.J. Evaluating the performance of the CCCI-CNI index for estimating N status of winter wheat. *Eur. J. Agron.* **2021**, *130*, 126346. [CrossRef]
120. Duan, B.; Fang, S.; Zhu, R.; Wu, X.; Wang, S.; Gong, Y.; Peng, Y. Remote estimation of rice yield with Unmanned Aerial Vehicle (UAV) data and spectral mixture analysis. *Front. Plant Sci.* **2019**, *10*, 204. [CrossRef]
121. Schirrmann, M.; Giebel, A.; Gleiniger, F.; Pflanz, M.; Lentschke, J.; Dammer, K.-H. Monitoring agronomic parameters of winter wheat crops with low-cost UAV imagery. *Remote Sens.* **2016**, *8*, 706. [CrossRef]
122. Wang, Y.; Wang, D.; Shi, P.; Omasa, K. Estimating rice chlorophyll content and leaf nitrogen concentration with a digital still color camera under natural light. *Plant Methods* **2014**, *10*, 36. [CrossRef]
123. Zhang, J.; Cheng, T.; Shi, L.; Wang, W.; Niu, Z.; Guo, W.; Ma, X. Combining spectral and texture features of UAV hyperspectral images for leaf nitrogen content monitoring in winter wheat. *Int. J. Remote Sens.* **2022**, *43*, 2335–2356. [CrossRef]
124. Xu, K.; Zhang, J.; Li, H.; Cao, W.; Zhu, Y.; Jiang, X.; Ni, J. Spectrum- and RGB-D-based image fusion for the prediction of nitrogen accumulation in wheat. *Remote Sens.* **2020**, *12*, 4040. [CrossRef]
125. Bausch, W.C.; Duke, H.R. Remote sensing of plant nitrogen status in corn. *Trans. ASAE* **1996**, *39*, 1869–1875. [CrossRef]
126. Cho, M.A.; Skidmore, A.K. A new technique for extracting the red edge position from hyperspectral data: The linear extrapolation method. *Remote Sens. Environ.* **2006**, *101*, 181–193. [CrossRef]
127. Chen, P.; Haboudane, D.; Tremblay, N.; Wang, J.; Vigneault, P.; Li, B. New spectral indicator assessing the efficiency of crop nitrogen treatment in corn and wheat. *Remote Sens. Environ.* **2010**, *114*, 1987–1997. [CrossRef]
128. Feng, W.; Zhang, H.-Y.; Zhang, Y.-S.; Qi, S.-L.; Heng, Y.-R.; Guo, B.-B.; Ma, D.-Y.; Guo, T.-C. Remote detection of canopy leaf nitrogen concentration in winter wheat by using water resistance vegetation indices from in-situ hyperspectral data. *Field Crops Res.* **2016**, *198*, 238–246. [CrossRef]

129. Barnes, E.; Clarke, T.; Richards, S.; Colaizzi, P.; Haberland, J.; Kostrzewski, M.; Waller, P.; Choi, C.; Riley, E.; Thompson, T. Coincident Detection of Crop Water Stress, Nitrogen Status and Canopy Density Using Ground Based Multispectral Data. In Proceedings of the Fifth International Conference on Precision Agriculture, Bloomington, MN, USA, 16–19 July 2000; p. 6.
130. Daughtry, C.S.; Walthall, C.; Kim, M.; De Colstoun, E.B.; McMurtrey Iii, J.E. Estimating corn leaf chlorophyll concentration from leaf and canopy reflectance. *Remote Sens. Environ.* **2000**, *74*, 229–239. [CrossRef]
131. Eitel, J.U.H.; Long, D.S.; Gessler, P.E.; Hunt, E.R. Combined spectral index to improve ground-based estimates of nitrogen status in dryland wheat. *Agron. J.* **2008**, *100*, 1694–1702. [CrossRef]
132. Lelong, C.C.D.; Burger, P.; Jubelin, G.; Roux, B.; Labbe, S.; Baret, F. Assessment of unmanned aerial vehicles imagery for quantitative monitoring of wheat crop in small plots. *Sensors* **2008**, *8*, 3557–3585. [CrossRef]
133. Chen, Z.; Miao, Y.; Lu, J.; Zhou, L.; Li, Y.; Zhang, H.; Lou, W.; Zhang, Z.; Kusnierek, K.; Liu, C. In-season diagnosis of winter wheat nitrogen status in smallholder farmer fields across a village using unmanned aerial vehicle-based remote sensing. *Agronomy* **2019**, *9*, 619. [CrossRef]
134. Brinkhoff, J.; Dunn, B.W.; Robson, A.J.; Dunn, T.S.; Dehaan, R.L. Modeling mid-season rice nitrogen uptake using multispectral satellite data. *Remote Sens.* **2019**, *11*, 1837. [CrossRef]
135. Yang, J.; Gong, W.; Shi, S.; Du, L.; Sun, J.; Song, S.L. Estimation of nitrogen content based on fluorescence spectrum and principal component analysis in paddy rice. *Plant Soil Environ.* **2016**, *62*, 178–183. [CrossRef]
136. Yl, Q.-X.; Huang, J.-F.; Wang, F.-M.; Wang, X.-Z.; Liu, Z.-Y. Monitoring rice nitrogen status using hyperspectral reflectance and artificial neural network. *Environ. Sci. Technol.* **2007**, *41*, 6770–6775.
137. Du, L.; Yang, J.; Sun, J.; Shi, S.; Gong, W. Leaf biochemistry parameters estimation of vegetation using the appropriate inversion strategy. *Front. Plant Sci.* **2020**, *11*, 533. [CrossRef] [PubMed]
138. Yang, J.; Du, L.; Gong, W.; Shi, S.; Sun, J. Estimating leaf nitrogen concentration based on the combination with fluorescence spectrum and first-derivative. *R. Soc. Open Sci.* **2020**, *7*, 191941. [CrossRef]
139. Yang, J.; Song, S.; Du, L.; Shi, S.; Gong, W.; Sun, J.; Chen, B. Analyzing the effect of fluorescence characteristics on leaf nitrogen concentration estimation. *Remote Sens.* **2018**, *10*, 1402. [CrossRef]
140. Yao, X.; Huang, Y.; Shang, G.; Zhou, C.; Cheng, T.; Tian, Y.; Cao, W.; Zhu, Y. Evaluation of six algorithms to monitor wheat leaf nitrogen concentration. *Remote Sens.* **2015**, *7*, 14939–14966. [CrossRef]
141. Wang, L.; Zhou, X.; Zhu, X.; Guo, W. Estimation of leaf nitrogen concentration in wheat using the MK-SVR algorithm and satellite remote sensing data. *Comput. Electron. Agric.* **2017**, *140*, 327–337. [CrossRef]
142. Liang, L.; Di, L.; Huang, T.; Wang, J.; Lin, L.; Wang, L.; Yang, M. Estimation of leaf nitrogen content in wheat using new hyperspectral indices and a random forest regression algorithm. *Remote Sens.* **2018**, *10*, 1940. [CrossRef]
143. Van Wittenberghe, S.; Verrelst, J.; Rivera, J.P.; Alonso, L.; Moreno, J.; Samson, R. Gaussian processes retrieval of leaf parameters from a multi-species reflectance, absorbance and fluorescence dataset. *J. Photochem. Photobiol. B-Biol.* **2014**, *134*, 37–48. [CrossRef]
144. Chlingaryan, A.; Sukkarieh, S.; Whelan, B. Machine learning approaches for crop yield prediction and nitrogen status estimation in precision agriculture: A review. *Comput. Electron. Agric.* **2018**, *151*, 61–69. [CrossRef]
145. Shah, S.H.; Angel, Y.; Houborg, R.; Ali, S.; McCabe, M.F. A random forest machine learning approach for the retrieval of leaf chlorophyll content in wheat. *Remote Sens.* **2019**, *11*, 920. [CrossRef]
146. Jacquemoud, S.; Baret, F. PROSPECT: A model of leaf optical properties spectra. *Remote Sens. Environ.* **1990**, *34*, 75–91. [CrossRef]
147. Feret, J.-B.; Francois, C.; Asner, G.P.; Gitelson, A.A.; Martin, R.E.; Bidel, L.P.R.; Ustin, S.L.; Le Maire, G.; Jacquemoud, S. PROSPECT-4 and 5: Advances in the leaf optical properties model separating photosynthetic pigments. *Remote Sens. Environ.* **2008**, *112*, 3030–3043. [CrossRef]
148. Jacquemoud, S.; Verhoef, W.; Baret, F.; Bacour, C.; Zarco-Tejada, P.J.; Asner, G.P.; Francois, C.; Ustin, S.L. PROSPECT plus SAIL models: A review of use for vegetation characterization. *Remote Sens. Environ.* **2009**, *113*, S56–S66. [CrossRef]
149. Verhoef, W. Light scattering by leaf layers with application to canopy reflectance modeling: The SAIL model. *Remote Sens. Environ.* **1984**, *16*, 125–141. [CrossRef]
150. Danner, M.; Berger, K.; Wocher, M.; Mauser, W.; Hank, T. Retrieval of biophysical crop variables from multi-angular canopy spectroscopy. *Remote Sens.* **2017**, *9*, 726. [CrossRef]
151. Sun, J.; Shi, S.; Yang, J.; Chen, B.; Gong, W.; Du, L.; Mao, F.; Song, S. Estimating leaf chlorophyll status using hyperspectral lidar measurements by PROSPECT model inversion. *Remote Sens. Environ.* **2018**, *212*, 1–7. [CrossRef]
152. Luo, Y.; Weng, E.; Wu, X.; Gao, C.; Zhou, X.; Zhang, L. Parameter identifiability, constraint, and equifinality in data assimilation with ecosystem models. *Ecol. Appl.* **2009**, *19*, 571–574. [CrossRef]
153. Combal, B.; Baret, F.; Weiss, M.; Trubuil, A.; Mace, D.; Pragnere, A.; Myneni, R.; Knyazikhin, Y.; Wang, L. Retrieval of canopy biophysical variables from bidirectional reflectance—Using prior information to solve the ill-posed inverse problem. *Remote Sens. Environ.* **2003**, *84*, 1–15. [CrossRef]
154. Thorp, K.R.; Wang, G.; West, A.L.; Moran, M.S.; Bronson, K.F.; White, J.W.; Mon, J. Estimating crop biophysical properties from remote sensing data by inverting linked radiative transfer and ecophysiological models. *Remote Sens. Environ.* **2012**, *124*, 224–233. [CrossRef]
155. Yang, G.; Zhao, C.; Pu, R.; Feng, H.; Li, Z.; Li, H.; Sun, C. Leaf nitrogen spectral reflectance model of winter wheat (*Triticum aestivum*) based on PROSPECT: Simulation and inversion. *J. Appl. Remote Sens.* **2015**, *9*, 095976. [CrossRef]

156. Li, Z.; Jin, X.; Yang, G.; Drummond, J.; Yang, H.; Clark, B.; Li, Z.; Zhao, C. Remote sensing of leaf and canopy nitrogen status in winter wheat (*Triticum aestivum* L.) based on N-PROSAIL model. *Remote Sens.* **2018**, *10*, 1463. [CrossRef]
157. Li, Z.; Li, Z.; Fairbairn, D.; Li, N.; Xu, B.; Feng, H.; Yang, G. Multi-LUTs method for canopy nitrogen density estimation in winter wheat by field and UAV hyperspectral. *Comput. Electron. Agric.* **2019**, *162*, 174–182. [CrossRef]
158. Verrelst, J.; Berger, K.; Rivera-Caicedo, J.P. Intelligent sampling for vegetation nitrogen mapping based on hybrid machine learning algorithms. *IEEE Geosci. Remote Sens. Lett.* **2021**, *18*, 2038–2042. [CrossRef]
159. Stagakis, S.; Markos, N.; Sykioti, O.; Kyparissis, A. Monitoring canopy biophysical and biochemical parameters in ecosystem scale using satellite hyperspectral imagery: An application on a Phlomis fruticosa Mediterranean ecosystem using multiangular CHRIS/PROBA observations. *Remote Sens. Environ.* **2010**, *114*, 977–994. [CrossRef]
160. Nagol, J.R.; Sexton, J.; Kim, D.-H.; Anand, A.; Morton, D.; Vermote, E.; Townshend, J.R. Bidirectional effects in Landsat reflectance estimates: Is there a problem to solve? *ISPRS J. Photogramm. Remote Sens.* **2015**, *103*, 129–135. [CrossRef]
161. Song, X.; Feng, W.; He, L.; Xu, D.; Zhang, H.-Y.; Li, X.; Wang, Z.-J.; Coburn, C.A.; Wang, C.-Y.; Guo, T.-C. Examining view angle effects on leaf N estimation in wheat using field reflectance spectroscopy. *ISPRS J. Photogramm. Remote Sens.* **2016**, *122*, 57–67. [CrossRef]
162. Lu, N.; Wang, W.; Zhang, Q.; Li, D.; Yao, X.; Tian, Y.; Zhu, Y.; Cao, W.; Baret, F.; Liu, S.; et al. Estimation of nitrogen nutrition status in winter wheat from unmanned aerial vehicle based multi-angular multispectral imagery. *Front. Plant Sci.* **2019**, *10*, 1601. [CrossRef]
163. Sun, T.; Fang, H.; Liu, W.; Ye, Y. Impact of water background on canopy reflectance anisotropy of a paddy rice field from multi-angle measurements. *Agric. For. Meteorol.* **2017**, *233*, 143–152. [CrossRef]
164. Huang, W.; Yang, Q.; Pu, R.; Yang, S. Estimation of nitrogen vertical distribution by bi-directional canopy reflectance in winter wheat. *Sensors* **2014**, *14*, 20347–20359. [CrossRef]
165. Ma, C.; Zhai, L.; Li, C.; Wang, Y. Hyperspectral estimation of nitrogen content in different leaf positions of wheat using machine learning models. *Appl. Sci.* **2022**, *12*, 7427. [CrossRef]
166. He, L.; Liu, M.-R.; Guo, Y.-L.; Wei, Y.-K.; Zhang, H.-Y.; Song, X.; Feng, W.; Guo, T.-C. Angular effect of algorithms for monitoring leaf nitrogen concentration of wheat using multi-angle remote sensing data. *Comput. Electron. Agric.* **2022**, *195*, 106815. [CrossRef]
167. Zhang, J.; Miao, Y.; Batchelor, W.D.; Lu, J.; Wang, H.; Kang, S. Improving high-latitude rice nitrogen management with the CERES-rice crop model. *Agronomy* **2018**, *8*, 263. [CrossRef]
168. Zhao, P.; Zhou, Y.; Li, F.; Ling, X.; Deng, N.; Peng, S.; Man, J. The adaptability of APSIM-wheat model in the middle and lower reaches of the Yangtze River Plain of China: A case study of winter wheat in Hubei Province. *Agronomy* **2020**, *10*, 981. [CrossRef]
169. Si, Z.; Zain, M.; Li, S.; Liu, J.; Liang, Y.; Gao, Y.; Duan, A. Optimizing nitrogen application for drip-irrigated winter wheat using the DSSAT-CERES-wheat model. *Agric. Water Manag.* **2021**, *244*, 106592. [CrossRef]
170. Cao, J.; Liu, X.J.; Tang, L.; Cao, W.X.; Zhu, Y. Model designing for suitable nitrogen index dynamics of rice and wheat. *Chin. J. Appl. Ecol.* **2010**, *21*, 359–364.
171. Zhang, X.; Friedl, M.A.; Schaaf, C.B. Global vegetation phenology from Moderate Resolution Imaging Spectroradiometer (MODIS): Evaluation of global patterns and comparison with in situ measurements. *J. Geophys. Res.-Biogeosci.* **2006**, *111*. [CrossRef]
172. Zheng, H.; Cheng, T.; Yao, X.; Deng, X.; Tian, Y.; Cao, W.; Zhu, Y. Detection of rice phenology through time series analysis of ground-based spectral index data. *Field Crops Res.* **2016**, *198*, 131–139. [CrossRef]
173. Zhang, M.; Zhu, D.; Su, W.; Huang, J.; Zhang, X.; Liu, Z. Harmonizing multi-source remote sensing images for summer corn growth monitoring. *Remote Sens.* **2019**, *11*, 1266. [CrossRef]
174. Shu, M.; Gu, X.; Zhou, L.; Xu, B.; Yang, G. Establishing NDRE dynamic models of winter wheat under multi-nitrogen rates based on a field spectral sensor. *Appl. Opt.* **2021**, *60*, 993–1002. [CrossRef] [PubMed]
175. Schlemmer, M.R.; Francis, D.D.; Shanahan, J.F.; Schepers, J.S. Remotely measuring chlorophyll content in corn leaves with differing nitrogen levels and relative water content. *Agron. J.* **2005**, *97*, 106–112. [CrossRef]
176. Kusnierek, K.; Korsaeth, A. Simultaneous identification of spring wheat nitrogen and water status using visible and near infrared spectra and powered partial least squares regression. *Comput. Electron. Agric.* **2015**, *117*, 200–213. [CrossRef]
177. Klem, K.; Zahora, J.; Zemek, F.; Trunda, P.; Tuma, I.; Novotna, K.; Hodanova, P.; Rapantova, B.; Hanus, J.; Vavrikova, J.; et al. Interactive effects of water deficit and nitrogen nutrition on winter wheat. Remote sensing methods for their detection. *Agric. Water Manag.* **2018**, *210*, 171–184. [CrossRef]
178. Berger, K.; Machwitz, M.; Kycko, M.; Kefauver, S.C.; Van Wittenberghe, S.; Gerhards, M.; Verrelst, J.; Atzberger, C.; van der Tol, C.; Damm, A.; et al. Multi-sensor spectral synergies for crop stress detection and monitoring in the optical domain: A review. *Remote Sens. Environ.* **2022**, *280*, 113198. [CrossRef]
179. Devadas, R.; Lamb, D.W.; Backhouse, D.; Simpfendorfer, S. Sequential application of hyperspectral indices for delineation of stripe rust infection and nitrogen deficiency in wheat. *Precis. Agric.* **2015**, *16*, 477–491. [CrossRef]
180. Raj, R.; Walker, J.P.; Pingale, R.; Banoth, B.N.; Jagarlapudi, A. Leaf nitrogen content estimation using top-of-canopy airborne hyperspectral data. *Int. J. Appl. Earth Obs. Geoinf.* **2021**, *104*, 102584. [CrossRef]
181. Wu, S.; Deng, L.; Guo, L.; Wu, Y. Wheat leaf area index prediction using data fusion based on high-resolution unmanned aerial vehicle imagery. *Plant Methods* **2022**, *18*, 68. [CrossRef]
182. Qiao, L.; Gao, D.; Zhang, J.; Li, M.; Sun, H.; Ma, J. Dynamic influence elimination and chlorophyll content diagnosis of maize using UAV spectral imagery. *Remote Sens.* **2020**, *12*, 2650. [CrossRef]

183. Xu, X.; Fan, L.; Li, Z.; Meng, Y.; Feng, H.; Yang, H.; Xu, B. Estimating leaf nitrogen content in corn based on information fusion of multiple-sensor imagery from UAV. *Remote Sens.* **2021**, *13*, 340. [CrossRef]
184. Yao, X.; Ren, H.; Cao, Z.; Tian, Y.; Cao, W.; Zhu, Y.; Cheng, T. Detecting leaf nitrogen content in wheat with canopy hyperspectrum under different soil backgrounds. *Int. J. Appl. Earth Obs. Geoinf.* **2014**, *32*, 114–124. [CrossRef]
185. Upreti, D.; Huang, W.; Kong, W.; Pascucci, S.; Pignatti, S.; Zhou, X.; Ye, H.; Casa, R. A comparison of hybrid machine learning algorithms for the retrieval of wheat biophysical variables from Sentinel-2. *Remote Sens.* **2019**, *11*, 481. [CrossRef]
186. Verger, A.; Baret, F.; Camacho, F. Optimal modalities for radiative transfer-neural network estimation of canopy biophysical characteristics: Evaluation over an agricultural area with CHRIS/PROBA observations. *Remote Sens. Environ.* **2011**, *115*, 415–426. [CrossRef]
187. Doktor, D.; Lausch, A.; Spengler, D.; Thurner, M. Extraction of plant physiological status from hyperspectral signatures using machine learning methods. *Remote Sens.* **2014**, *6*, 12247–12274. [CrossRef]